IEEE Journal of Microwaves

Received 17 November 2022; accepted 22 November 2022. Date of publication 23 December 2022;
date of current version 6 January 2023.

Digital Object Identifier 10.1109/JMW.2022.3226125

Frontiers in Flexible and Shape-Changing Arrays

AUSTIN C. FIKES [1] (Member, IEEE), MATAN GAL-KATZIRI [1,3] (Member, IEEE), OREN S. MIZRAHI [1] (Student Member, IEEE), D. ELLIOTT WILLIAMS [1,2] (Member, IEEE), AND ALI HAJIMIRI [1] (Fellow, IEEE)

(Invited Paper)

[1]Department of Electrical Engineering, California Institute of Technology, Pasadena, CA 91125 USA
[2]Department of Engineering, Hofstra University, Hempstead, NY 11549 USA
[3]Department of Electrical Engineering, Ben-Gurion University of the Negev, Beer-Sheva 8410501, Israel

CORRESPONDING AUTHOR: Austin C. Fikes (e-mail: afikes@caltech.edu).

Author order is alphabetical with the exception of the principal investigator. *(All authors contributed equally to this work.)*

ABSTRACT Shape-changing arrays are an emerging frontier of phased array development. These arrays fold, conform, and flex dynamically as they operate. In this work we describe the technology developments which have enabled their creation and use. We present the theoretical implications of aperture change for arrays and methods for taking advantage of these aperture changes. We discuss existing shape-changing array components and systems. Operation techniques for shape-changing arrays, including new results demonstrating a method for determining the shape of an asymmetrically bent flexible array using only the mutual coupling between elements, are shown. Finally, we present a comparison of shape-changing systems across a variety of physical and electrical metrics.

INDEX TERMS MTT 70th Anniversary Special Issue, shape-changing array, flexible phased array, integrated circuit based array, deployable, origami, flexible electronics, stretchable electronics.

I. INTRODUCTION

Over the last two decades, the introduction of phased arrays built with silicon-based microwave and mm-wave integrated circuits resulted in a paradigm shift in the nature, variety, economics, complexity, and breadth of applications of phased arrays. Prior to silicon-based radio frequency integrated circuits (RFICs), array architectures were mostly limited by the cost, size, and component count needed to implement each element. Compact, multi-function systems were preceded by mechanically steered, rigidly conformal arrays which have been used in aerospace applications for decades [1], as well as frequency steered arrays [2], [3] and bulky discrete component arrays with modest element counts [4], [5]. A survey of design and operation techniques for these early arrays is found in [6]. Over time compound semiconductor (e.g. GaAs) based monolithic microwave integrated circuits began to reduce the size of phased array implementations [7], [8], however the lower yield and higher cost of the compound semiconductor solutions limited the complexity and architectural choices of such arrays.

Silicon-based RFICs unlocked the planar integrated-circuit-based phased arrays that have become a pillar of emerging communication networks [9]. This transition began with the introduction of key functional units and front-end systems built on silicon-based technologies starting in year 2000 [10], [11], [12], [13], which was shortly followed by fully integrated, multi-element phased array receivers [14], [15], [16], [17] and transmitters [18], [19] at 24 GHz. Subsequent demonstrations of building blocks at 60 GHz in 2005 [20], [21] and fully integrated phased arrays transceivers with on-chip frequency synthesis and antennas at 77 GHz in 2006 [22], [23] further accelerated this transition. In 2008 several K_a-band array RFICs were demonstrated [24], [25]. The ability to integrate multiple functions such as frequency synthesis, clock recovery, data re-timing, and time or frequency multiplexing on the same die, enabled scalable modular design

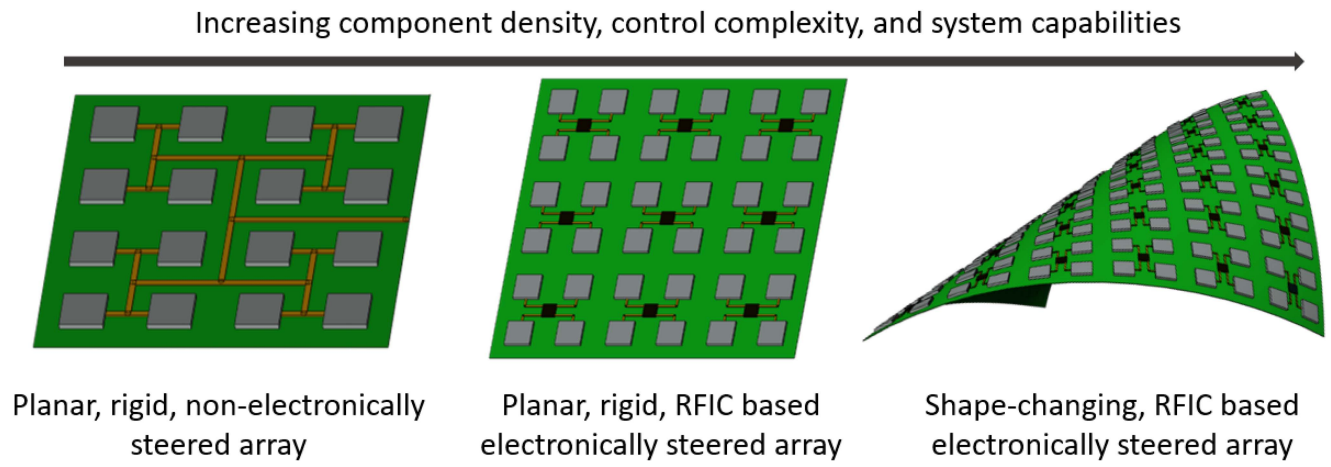

FIGURE 1. **Phased arrays have evolved from static pattern, rigid arrays to multi-function, electronically steered, integrated circuit based arrays. The next frontier for array development is dynamically shape-changing arrays.**

without the need for distribution of high frequency signals across the array [26]. In 2009, integration of many element-drive circuits in a single chip was shown at 60 GHz [27], [28], [29]. The new paradigm was rapidly picked up by a large number of more complex phased arrays systems that were developed later to serve a broad range of applications [30], [31], [32], [33], [34].

While planar mm-Wave phased arrays have cemented their position in communication systems, the future of IC-based arrays is not solidified in frequency, application, or form factor. The operation frequency of these arrays climbs ever upward, even to the optical range with silicon photonics-based optical phased arrays [35], [36], [37] and new circuit techniques enabling low terahertz frequency arrays in CMOS [38], [39]. Integrated circuit-based phased arrays are now being used in spectroscopy [40], wireless power transfer [41], and ranging and sensing [42]. In this paper, we present how the these silicon integrated ICs have led to an ongoing evolution in form factor. Shape-changing phased arrays, which encompass mechanically flexible, foldable, multi-faceted, or stretchable arrays, are one of the promising new frontiers of array development. The future "asymptote" of this development path is a multi-purpose, high-bandwidth array which is as flexible and light as a sheet of paper. While the path to this asymptotic array is dictated by the realities of material limitations and electromagnetic principles, it is a vision worth aspiring to.

Arrays formed by thin flexible substrates with small and lightweight components are conducive to deployable or conformal systems which are mechanically reconfigurable through flexing, folding, or stretching. These capabilities allow arrays to dynamically conform to changing surfaces such as the human body as active fabric, flutter in the wind like sails, deploy rapidly to replaced damaged communication infrastructure, or deploy in space for sensing, communications, or power transfer. Both smaller arrays for satellite communications [43], [44] and ultra-large scale arrays for space-based solar power [45], [46], [47] require the light weight and physical reconfigurability offered by shape-changing arrays. Wearable systems with wireless communication require flexible antennas and would benefit from the electronically steered beams and reconfigurable patterns offered by shape-changing phased arrays. For example, a future stretchable shape-changing array could bring additional capabilities to wearable on-body wireless communications systems such as [48]. Shape-change itself can also be intentionally leveraged to dynamically alter antenna properties such as aperture size or field of view. In [49], shape-change is used to add measurement diversity and improve image quality for a microwave imaging array. The progression from rigid, static pattern arrays to electronically steerable, shape-changing arrays is shown in Fig. 1.

Despite its potential there are several significant challenges created by the non-rigid form factor. It is immediately obvious that changing the relative positions of elements within an array requires the element excitation phases to be adjusted in order to compensate and maintain desired beam properties. Additionally, as the array changes shape, its total aperture stretches, shrinks, or curves. These aperture changes modify the achievable directivity, field of view, and side-lobe level of the array. There are also component level changes that accompany array shape changes. Element patterns may be altered as the local ground plane curves. Even transmission line propagation characteristics may be changed as their conductors and dielectric are bent or separated. These issues are depicted in Fig. 2(a)–(d).

The shape-changing array hardware discussed in this work are suitable for frequencies ranging approximately from hundreds of MHz up to hundreds of GHz. This is not a strict range but represents boundaries outside of which other solutions may be preferred. At frequencies below this range arrays are so large that there is little advantage in having elements physically connected whether through rigid or shape-changing means. At the upper end of this range array apertures are small even at high element counts and thus have less need for shape-change. Although shape-changing arrays above one hundred GHz built entirely from integrated circuits with on-chip

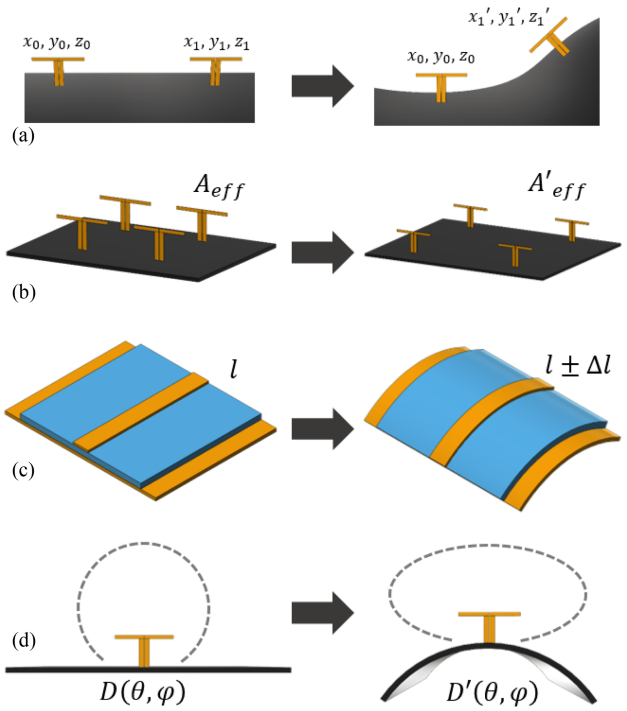

FIGURE 2. Electromagnetic changes induced by array shape changes. (a) Relative position of array elements changes. (b) Aperture size changes. (c) Transmission line propagation characteristics may be altered when bent or stretched. (d) Individual radiator element patterns may change as array shape changes.

radiators are conceivable, their hypothetical implementations would differ significantly from the arrays presented here. While the hardware solutions may be suited to a specific frequency range, the analysis of shape-changing apertures presented in Section II and operation techniques in Section IV are frequency independent and could even be adapted to arrays for non-electromagnetic waves. While fully integrated, flexible microwave arrays are a recent development, ultrasound flexible arrays have been an active area of research for several decades [50], [51], [52].

The family of shape-changing arrays is broader than just those built on flexible substrates. While "flexible" refers specifically to arrays which change shape with approximately constant Gaussian curvature [53], other shape-changing array implementations include "origami" or "kirigami" [54] folding of rigid or semi-rigid panels [55] (also referred to as multi-faceted arrays) and stretchable arrays which both bend and change Gaussian curvature. These shape-changing array varieties share many system components and operation techniques but differ in both obvious and subtle ways in implementation and electromagnetic implications. It should be noted that static, rigidly conformal arrays (such as [1]), long used for aerospace applications, are a separate category from the fully integrated, flexible and dynamically shape-changing arrays on which this work focuses.

This paper presents theory, prototypes, and operation techniques for shape-changing arrays using silicon based integrated circuits. Section II presents the mathematical ramifications of shape change and categorizes different shape change approaches in order to study their implications for RF and system design and performance. Section III presents several prototype flexible array components and systems. Section IV describes operation techniques for shape-changing arrays including closed loop array focusing and a method for determining array shape using mutual coupling measurements under non-constant curvature settings.

II. SHAPE-CHANGING APERTURES

As an array's shape is altered, the relative positions and orientations of its elements change. In a sense, it becomes a new array; changes in coupling alter the port impedances and element patterns, changes in orientation disrupt the envelope imposed by the element pattern on the array pattern, and changes in the element locations alter the interference pattern of the radiation in both the near and far-fields. However, these changes can be mitigated through coupling-robust power amplifiers, elements with smooth and wide beam-width patterns, and effective beam-steering algorithms. Shape change also fundamentally alters the array aperture and thus its maximum gain and steering range. Even the previously described asymptotic array with ideal mechanical shape-change properties is subject to the electromagnetic consequences of aperture change. In this section the electromagnetic advantages and mathematical requirements for arbitrary shape-change and the resulting consequences for RF performance and system implementations are explored.

A. THEORETICAL CONSEQUENCES OF SHAPE CHANGE

Geometric optics provides a bound for the aperture of a dense high-element-count phased array [56]: thus the maximum aperture of an array in a given direction is proportional to its cross-sectional area. Therefore the aperture of a planar array decreases at large steering angles, limiting its steering range. A spherical array, however, can radiate uniformly in any direction. This increased steering range comes at the cost of reduced maximum gain when compared to a planar array with the same active array area; the cross-sectional area is reduced and some elements point away from the desired beam direction and cannot be used.

Fig. 3 shows the maximum gain at different steering angles for several simple array geometries. A spherical array will have 6 dB less maximum gain, and a -3 dB steering range three times larger than a planar array of the same active area. There is thus a fundamental trade-off between the maximum gain and steering range of an array that is determined by the array geometry. Controlled mechanical shape change allows a single array to circumvent this trade-off by altering its aperture to the configuration best suited for the desired task. Conversely uncontrolled shape change, such as active fabrics or fluttering arrays, will subject the array to dynamic changes in its maximum achievable gain and steering range that must be accounted and corrected for.

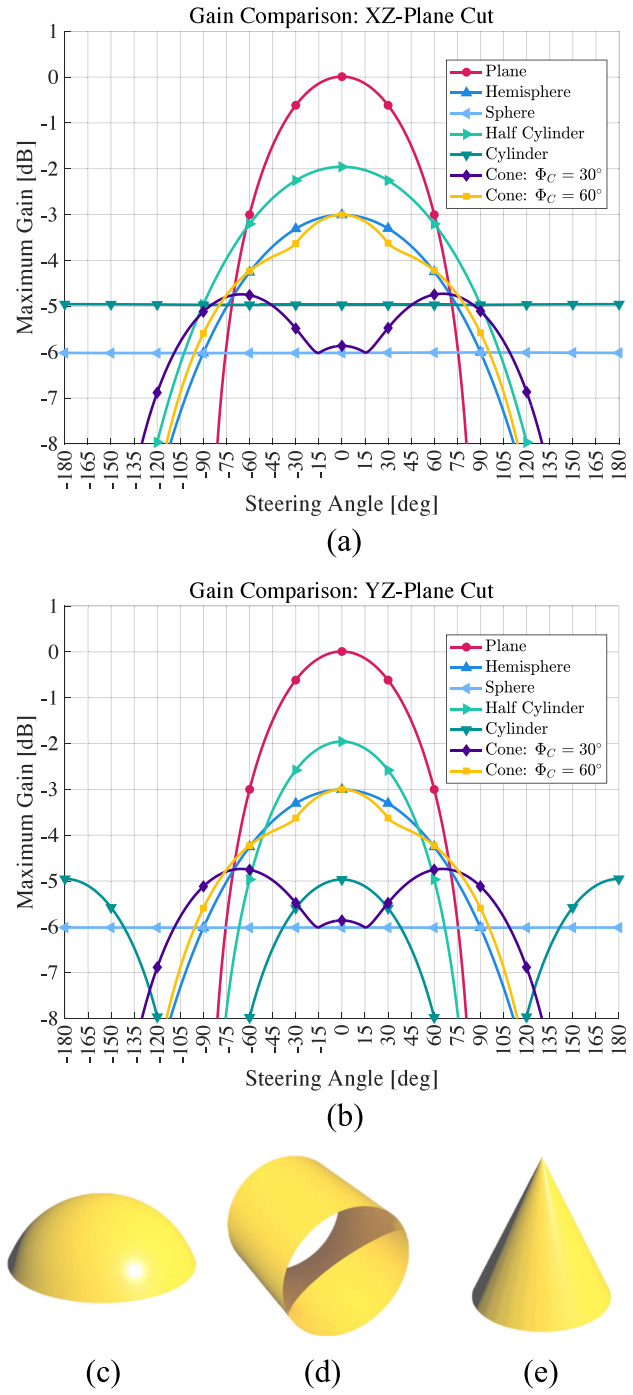

FIGURE 3. **The geometry of an array determines its maximum cross-sectional area, aperture, and gain at different steering angles. Maximum gain of different geometries with equal surface area in the (a) *xy*- and (b) *yz*-planes. The gains are normalized to the maximum gain of the planar array. Cylinders are curved in the *xy*-plane. Example geometries: (c) hemisphere, (d) cylinder, (e) cone.**

B. LIMITATIONS DUE TO GAUSS'S THEOREMA EGREGIUM

Gauss's *Theorema Egregium* law is of preeminent importance to shape-changing arrays. The theorem states that "the Gaussian curvature of a surface is invariant under local isometry" [53]. Thus, if the distances between points on an array's surface cannot change, then the array cannot alter its Gaussian curvature. The contrapositive also holds; in order for a array to change its Gaussian curvature, the spacing between elements in the array *must* change. These facts have major consequences for shape-changing arrays as the Gaussian curvature is a measure of a surface's curvature in multiple directions; planar arrays have zero Gauss curvature while spherical arrays have a Gauss curvature inversely proportional to their radii.

Therefore, a planar array comprised of materials that are *flexible* but not *stretchable*, such as polyimide and copper, can only morph into shapes with zero Gauss curvature. A helpful analogy is that such arrays can only take on shapes that a thick sheet of paper can without folding or crumpling. This limitation in possible geometries is an advantage with respect to the array's structural rigidity and the ability to reconstruct the array shape from measurements on the surface. However, it precludes such flexible arrays from taking on arbitrary shapes and increasing the steering range in multiple directions. The most common flexible phased arrays fall into the constant curvature category.

C. CATEGORIES OF SHAPE-CHANGING ARRAYS

In order for a shape-changing array to take on *arbitrary* configurations, the distance between its elements *must* change. Stretchable substrates can alter their atomic lattice spacing or polymer chain orientations to directly change the material length. However, arrays of non-stretchable materials can also alter the effective element spacing by using folds or cuts to respectively hide extra material on the array's interior or introduce gaps on the array surface.

As only one geometric configuration can have an ideal $\frac{\lambda}{2}$ spacing, it is helpful to categorize shape-changing arrays based on whether they reduce or increase the average spacing compared to this ideal. Therefore, there are four ways that an array can take on arbitrary geometries, depending on the change in spacing and the material properties: an array can be compressed, stretched, folded, or cut. Each of these methods have important system design and performance implications. Fig. 4 contains a conceptual diagram of the categories of arbitrary shape-changing phased arrays and Fig. 5 depicts different implementations of shape-changing phased arrays and sensor arrays. To the authors' best knowledge a stretchable/compressible active antenna array has not yet been explored in the literature.

By definition, compressible and foldable arrays shrink the average spacing. This has the effect of both decreasing the effective aperture of the array and increasing the element coupling. Higher coupling increases the sensitivity of the element impedance to the steering angle, thus degrading power amplifier output power, linearity, and efficiency [61], [62]. Coupling can also alter the active element pattern [63]. Foldable arrays can maintain the surface spacing while decreasing the average spacing by hiding active elements in the folds. While this mitigates the effect of increased coupling, it degrades the Effective Isotropic Radiated Power (EIRP) as the aperture is still reduced as are the number of elements in the array.

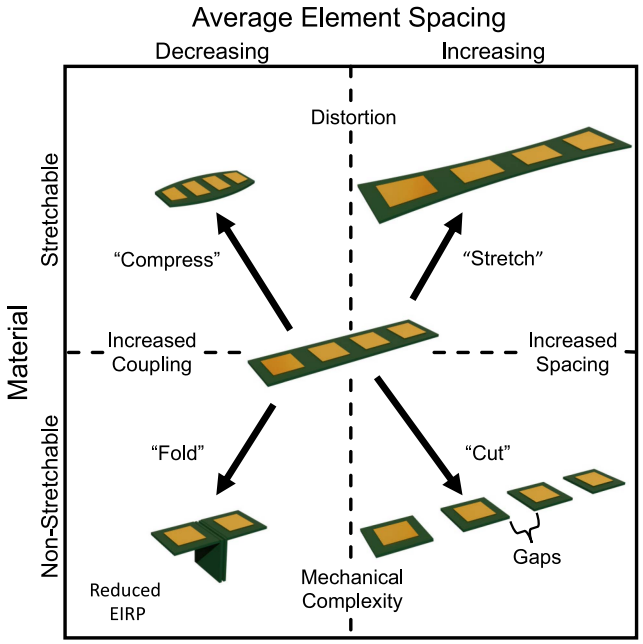

FIGURE 4. Categories of arbitrary shape changing phased arrays.

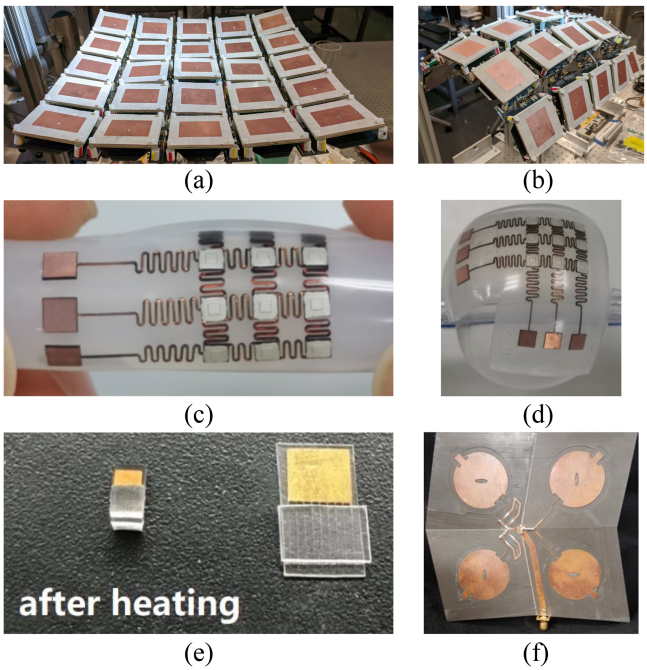

FIGURE 5. Examples of different kinds of shape changing arrays: Cut phased array in (a) planar and (b) cylinder configurations [57], stretch sensor array (not a phased array) in (c) cylinder (d) and spherical configurations [58]. Reproduced with permission. (e) A microelectrode array fabricated using irreversible compression [59], reproduced with permission. (f) deployable antenna array in planar configuration [60], reproduced with permission.

In contrast, cutting or stretching the array increases the average spacing between elements. Thus a densely-packed array becomes sparse, with the associated increase in grating lobes and reduction in fill-factor. Fig. 6 demonstrates the sidelobe degradation induced by shape change by comparing

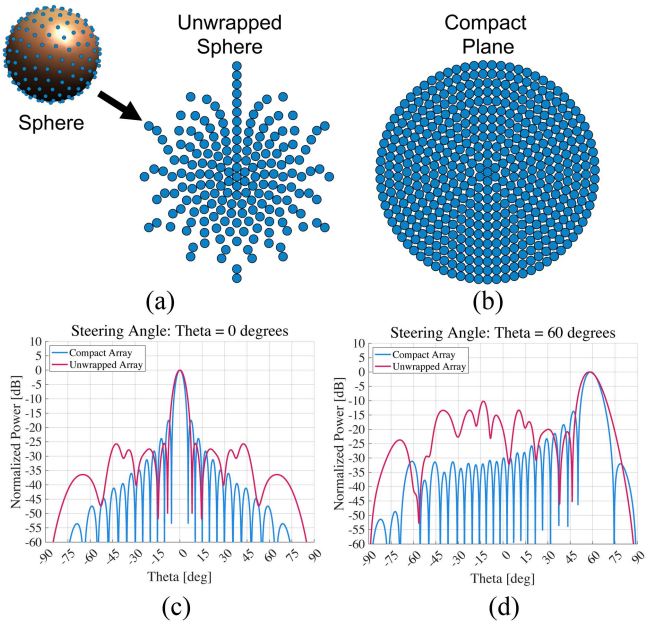

FIGURE 6. Shape-change modifies the spacing between elements, introducing grating lobes. (a) A densely packed spherical array is unwrapped to a planar configuration. (b) A densely packed circular array with the same aperture. A comparison of the grating lobes when beams are steered to (c) $\theta = 0°$ and (d) $\theta = 60°$. Amplitude tapering and phase optimization have not been used in either array to suppress side lobe levels. As can be seen, the grating lobe performance is degraded by shape-change.

the pattern of a densely-packed circular array to that of a densely-packed spherical array that has been stretched to form a planar circular array with the same aperture.

D. IMPLEMENTATION CHALLENGES AND OPPORTUNITIES

While a fold or cut array's radiators can themselves can be rigid, the connections between them must be flexible to support the change in distances. Interconnects crossing folds must be flexible and reliable enough to handle the sharp bends required for folding as seen in Fig. 4(f). Alternatively, flexible cables can be used to create direct element to element connections that span gaps that grow and shrink. This approach is well suited to systems consisting of independent tiles held in position by a mechanical backbones as in [57]. Designing these backbones to securely hold tiles in multiple desired configurations despite the inherently large numbers of degrees of freedom is an area of active structural research [64].

Cut based shape changing arrays have a unique property that can be exploited to enhance array performance; the gaps introduced provide additional area on the surface of the array. As shown in Fig. 7, these gaps can be filled with flexible passive sheets (meta-gaps) that are stored behind the array when the gaps disappear. These structures are capable of reducing the side-lobe levels of a lambda-spaced array by at least 2 dB [65].

In the case of stretching and compressing, the array substrate material distorts to alter the distances along the surface.

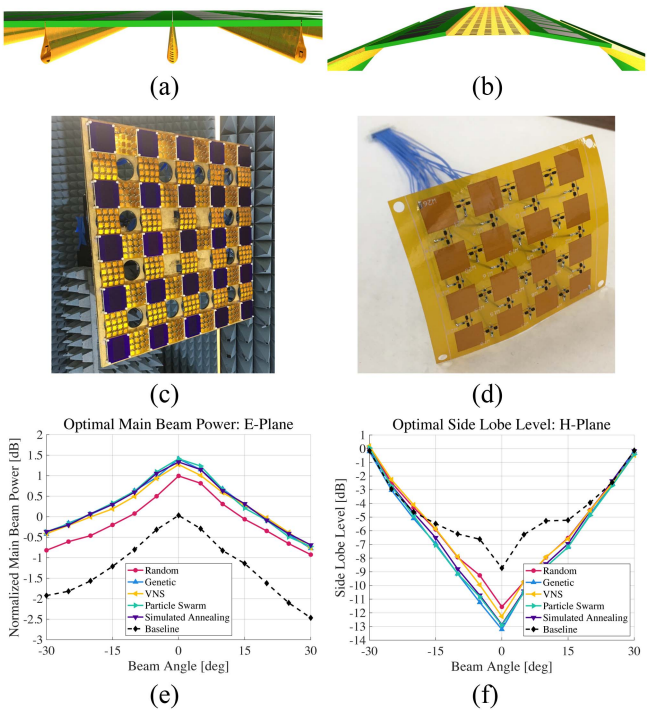

FIGURE 7. **Meta-gaps can be placed in the gaps of a cut array to alter the array characteristics [65]. The copyright holder of these figures is the European Microwave Association. Originally published in September 2022 by D.E. Williams and A. Hajimiri. (a) Meta-gaps stored behind array when gaps do not exist. (b) Deployed meta-gaps. (c) A lambda-spaced demonstration array with meta-gaps between antennas. (d) A flexible switchable meta-gap sheet. Optimized (e) main beam power and (f) side-lobe level of array using switchable meta-gaps.**

Therefore conductive traces, transmission lines, and antennas on the surface will be distorted by the shape change. Traces and transmission lines must either include meandering paths to compensate as in Fig. 5(d), or be constructed out of flexible conductive material such as liquid metal-embedded elastomers [66]. The changes in conductor dimensions requires antenna and transmission line performance to be robust to distortion or utilize distortion to achieve a desired effect such as frequency and pattern reconfigurability. For example, this distortion could be leveraged to create meta-materials that only resonate and alter array performance at the operating frequency in a particular configuration.

III. FLEXIBLE PHASED ARRAYS

Flexible non-stretchable phased arrays are a special subclass of shape-changing arrays which have experienced significant interest recently. This is partly due to their mechanical simplicity and strength combined with the availability of commercial flexible substrates compatible with custom RFIC-based arrays. In this section we will discuss the building blocks of such arrays and their associated trade-offs.

A. RADIATOR DESIGN

The electrical and mechanical properties of the radiator play a significant role in the overall behavior of shape-changing phased arrays. The circuit components of a phased array (ICs, passives, transmission lines, etc.) can be regarded as mostly planar and low profile. However, efficient, directional, and moderate/high bandwidth radiators typically have a non-negligible depth [56] set by the radiated wavelength. Added depth is usually not an issue for multi-faceted shape changing arrays built from rigid sub modules with dynamic interconnects [72], however for *flexible* shape-changing arrays, the design of suitable radiators can be a challenge. It is also common for flexible arrays to be heavily mass-constrained given that low weight is a priority for applications such as space deployable [45] or bio-conformal arrays.

Fig. 8 illustrates several radiators that have been used in flexible arrays. As array antennas are usually directional, back-radiation from them is undesirable for efficiency, interference, and/or safety reasons, and standard omni-directional or bi-directional flexible radiators like in Fig. 8(a) [67] cannot be used. The addition of reflectors or a ground plane behind the radiators forces a gap that increases the antenna's height and mass. A straightforward implementation could use dipole-like radiators, fabricated on a thin film, and mounted perpendicular to a ground plane sheet, as shown in the folded-dipole of Fig. 8(b) [68]. This design achieves good efficiency and has low mass, but is mechanically less suitable for deployable and dynamic array applications, due to its rigidity in one direction.

An improved design utilizes a curved flexible glass-fiber sheet as a support for the thin antenna structure, as in Fig. 8(c). In this manner, the support provides additional mechanical stability and allows the radiators to be bent towards the ground plane ("collapsed") while the antenna is flattened then rolled in storage [69]. The stored antennas "pop-up" to their deployed state and operate as standard reflector-backed dipoles. Design simplicity favors single deployment, especially for inaccessible environments, such as space. The antenna in [69] is well suited for flexible arrays that are folded, rolled, and stacked prior to use or between uses. While a directional antenna without a ground plane is possible, the dipole antennas described above and the patch antennas described below both use a ground plane. In addition to facilitating directionality, the ground plane provides isolation between components or objects on the backside of the array and its radiators. While these properties are advantageous, especially for conformal applications, a continuous ground plane can restrict flexibility. In [69] a meshed ground plane is used to provide mechanical relief when flexing. Fig. 9 shows the pop-up dipole antenna's mesh grid. The mesh (0.2 mm width and 1 mm pitch) is sufficiently sub-wavelength such that antenna operation is not affected.

Alternatively, patch antennas have been utilized in flexible phased arrays in order to streamline the antenna profile at the cost of bandwidth and deteriorated inter-element isolation. In general, patch antennas are compact, ground-plane backed structures with single-side radiation patterns that are favorable to shape-changing applications. For example, in Fig. 8(d), radiator patterns are etched onto a thin, copper-clad laminate

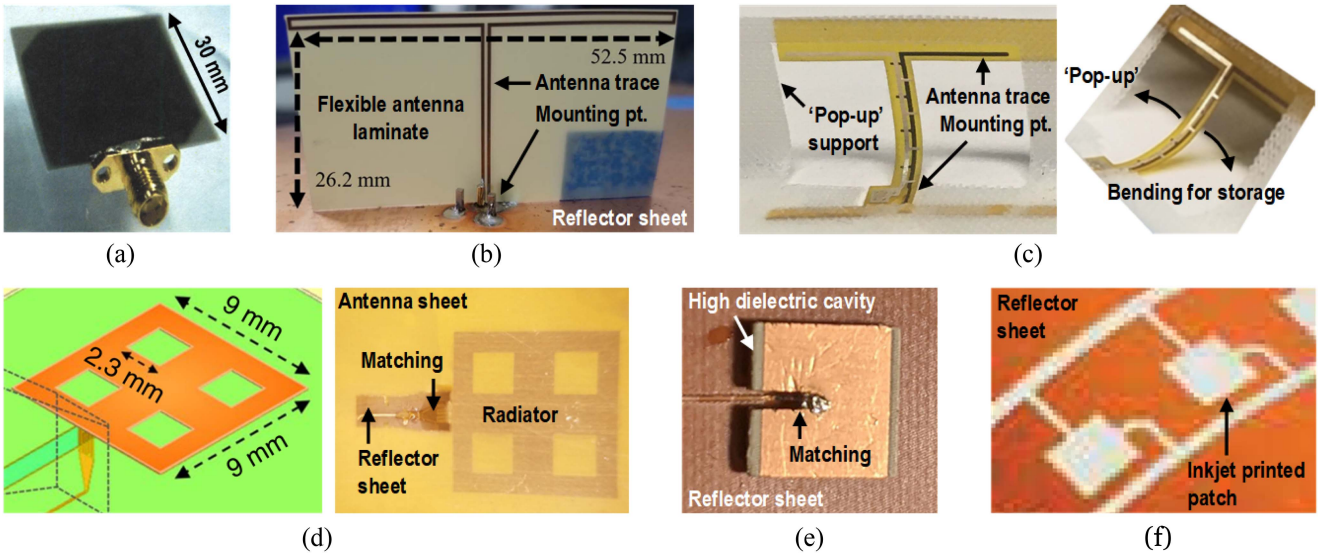

FIGURE 8. Examples of flexible-array compatible antennas: (a) Undesirable bi-directional patch reprinted with permission from [67], (b) vertical folded dipole antenna [68] licensed under CC BY-NC-ND 4.0, (c) 'pop-up' approach for packaging of vertical antennas [69], (d) air-gap patch antenna [47] reprinted with permission, (e) dielectric patch antenna [70], and (f) Inkjet-printed antenna reprinted with permission from [71].

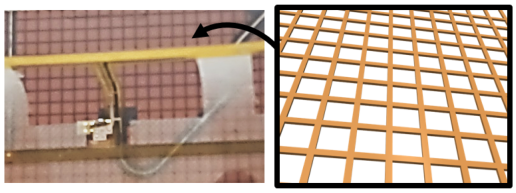

FIGURE 9. Mesh ground of [69] enables flexibility and reduces mass.

that is separate from the array circuit board. The antenna sheet is aligned and soldered onto the flexible reflector body, then lifted to provide the patches an air gap from ground which acts as the radiator cavity. The vertical antenna feed trace performs the required impedance matching—in this case to 50 Ω. Air gap patch sheets are efficient with a reasonable bandwidth of 10%–15% [47], but require a support frame to hold them taut above the ground surface. If the support frame is collapsible, the whole structure can be rolled up to the arc length difference between the antenna and reflector sheets, due to shear stress induced by the different radii of curvature. If greater flexibility is required, discrete dielectric patches can be utilized as illustrated in Fig. 8(e), at a cost of mass and/or loss compared to air gap patches [70]. In higher frequency ranges, where the flexible substrates are thick enough to be a meaningful fraction of a wavelength, inkjet-printed antennas have been successfully demonstrated as shown in Fig. 8(f) [71].

Radiators for flexible and shape-changing arrays are at risk of experiencing input match de-tuning and radiation pattern variations as their shape is altered. Local ground plane shape deformation and distance changes to neighboring elements are likely culprits. In [73], the patterns of dipole antennas in a flexible array were shown to be somewhat insensitive to bending. Patch antennas, which are often modeled as lossy cavity resonators [74], and other high Q-factor antennas with narrow bandwidths could be more sensitive to shape deformation and thus more at risk for de-tuning and pattern alteration. Further antenna bend sensitivity analysis and the development of a variety of bend insensitive array radiators could inform the design of future shape-changing arrays.

B. FLEXIBLE ARRAYS

The radiators discussed above do not by themselves provide any means of phase delay adjustment as required in active, electronically steered arrays. In rigid phased arrays, signal conditioning is managed by accompanying electronic circuitry that is not necessarily nearby the radiators. This can be done either by vertical integration with additional control boards [77] or by the use of a separate central processing unit that has individually controlled outputs for each of the radiators. Naturally, vertical integration with rigid control boards is infeasible for flexible arrays. In [78], for example, The radiators are connected with RF cables to additional rigid circuitry that lies behind the antenna sheet and performs signal conditioning. Even though the radiators themselves may be implemented on a flexible substrate, such a structure requires a physical support and is better suited to static, conformal applications.

In [49], the authors demonstrate an important practical advantage of a mechanically shape-changing array with rigid radiators, namely—control of the field-of-view of the radiation pattern. This feature is particularly useful in imaging systems, where it can add a fundamentally independent modality to diversity measurement methods, in order, for example, to handle highly reflective planar interference, or to reduce the effects of specular reflections.

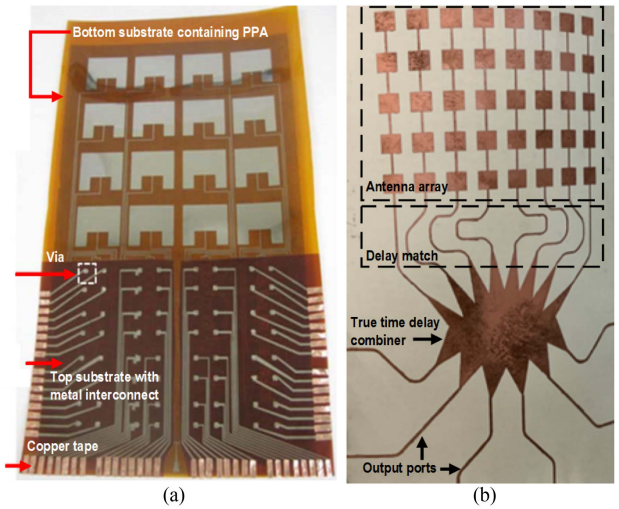

FIGURE 10. **Flexible phased arrays with timing control placed on the same sheet to the side of the radiators, using (a) phase shifters [75] reprinted with permission or (b) true-time delay Rotman lense [76] licensed under CC BY 4.0.**

A different and more straightforward approach is to add the timing adjustment circuitry on the same flexible sheet as the radiators, as demonstrated in various flexible back-scatters and other low-power IoT systems. In [75], 16 inkjet-printed antennas form a 4 × 4 array operating at 5 GHz, as illustrated in Fig. 10(a). Due to space and complexity constraints, the phase shifter resolution is set to 2-bit only, and scan angle is limited to 34°, but the implementation's simplicity enables extreme flexibility. In [76], a more sophisticated central control of back-scatter array receive direction uses the outputs of a Rotman lens as a true-time delay to the different output ports (Fig. 10(b)). The array is implemented on a flexible liquid crystal polymer (LCP) and is further used to combine DC down-converted signals at each output port, without on-board dynamic signal control. There are certain limitations in placing additional electronics on the same side of the antenna array. Mainly, the use of excess area—roughly the same as the radiators—resulting a larger system footprint with a limited scalability.

While the arrays described above are flexible phased arrays, they lack either the scalability, resolution, power, or versatility that a fully functional array could offer. The most versatile approach is to directly integrate the electronic circuitry throughout and place it in close proximity to the radiators themselves. Namely, to embed the antenna sheet with RFICs that reduce the component count and offload most of the signal conditioning tasks from a main processing unit without compromising the flexibility or mass of the array. This feature is critical in ultralight applications, e.g. [79], [80], where the system mass determines the system viability [81]. A significant advantage of this architecture is that it naturally lends itself to distributed power supply schemes—e.g., local energy supply from photovoltaic cells to nearby RFICs—to eliminate the need of heavy/rigid low-resistivity DC power traces.

A fully contained flexible RF phased array tile intended for space-based wireless power transmission was demonstrated in [47]. The system, illustrated in Fig. 11 performs solar-to-RF power conversion and consists of three major parts. Light is concentrated in solar cells using parabolic reflectors that convert it to DC power (Fig. 11(a)). DC power is then converted to RF using a power converter RFIC that is placed on a flexible sheet carrier (Fig. 11(b)). As illustrated in Fig. 11(c), this RFIC provides complex system functionality. It can be digitally program to use a reference clock in the 10 MHz to 300 MHz range. The clock serves to synchronize multiple tiles in larger implementations of the modular array architecture. The clock is used to synthesize a 2.5 GHz on-chip reference that is used by each of the 16 independent channels to generate independently controlled outputs at 10 GHz. The signal path of each output channel in the RFIC provides individual phase and amplitude control, and power amplification that is the DC-RF power conversion. The RFIC performs additional functions such as temperature and signal monitoring, closed-loop stabilization of the PA operating point, and independent pulse-modulated phase change sequences that facilitates sophisticated modes of operation.

The RFIC outputs are routed through the flexible carrier to a separate antenna sheet with 4 × 4 patch radiators, as illustrated in Fig. 11(d). The whole assembly consists of a fully contained phased array with an ultra-low areal mass density less than 100 mg/cm^2. In [82], sixteen 4 × 4 phased array tile patterns from [47] were used to form a modular, 256-element flexible phased array, with beam-steering and static deformation-correction capabilities, as shown in Fig. 12. The larger array employs RFICs with on-chip delay-locked loops (DLL) that enables a robust operation of multiple tiles in concert.

A larger implementation of a continuously flexible phased array presented in a more streamlined design was demonstrated in [70] where the platform that was used in [82] was fitted with dielectric patch antennas instead of a single sheet. Fig. 13 illustrates how 16 sub-module tiles were combined to form a 256-element 30 cm × 30 cm array. The discrete radiators greatly increase the system flexibility: functional operation of single- and doubly-curved array with bend radius less than 23 cm (bend angle, $\theta \approx 75^\circ$) was demonstrated. This large and flexible phased array was also deployed and operated outdoors as proof of its robustness.

The previously described large-scale flexible arrays are intended for wireless power transfer, smaller scale flexible arrays could have a future role in satellite communication. Two fully integrated RFIC-based mm-Wave phased arrays were recently published with space-borne communication as their intended application. A tileable, fully integrated flexible phased array receiver was shown in [43]. The 32 element array operates at 19 GHz, uses inkjet printed conductors and is designed for future scalability. At 28 GHz, [44] shows an 32 element fully integrated transmitter array built on a flexible LCP substrate. This array was used to demonstrate data transmission up to 2.5 Gbps with 32 APSK.

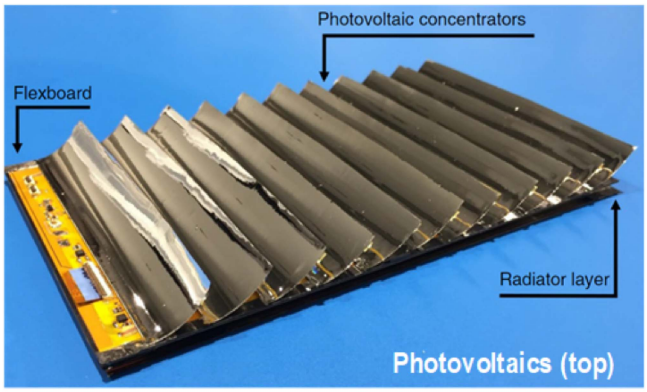

(a)

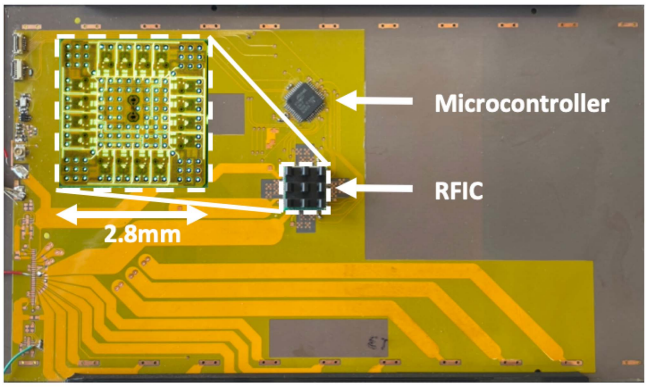

(b)

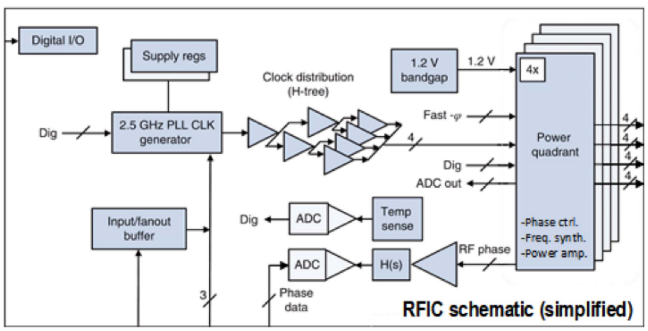

(c)

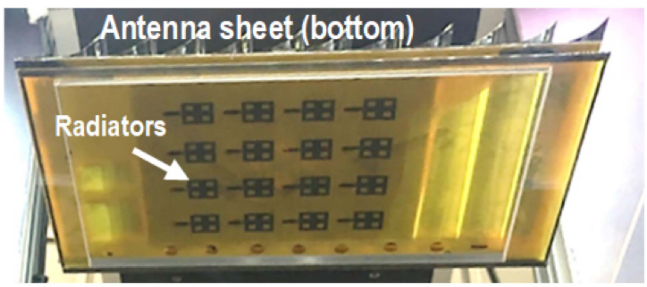

(d)

FIGURE 11. A fully contained 4 × 4 phased array with integrated solar power supply [47]. (a) Top view of photovoltaic concentrators, with (b) a DC-RF converter RFIC below them. (c) RFIC simplified schematics. (d) Bottom view of the antenna side of the integrated power converter tile. Images reproduced with permission.

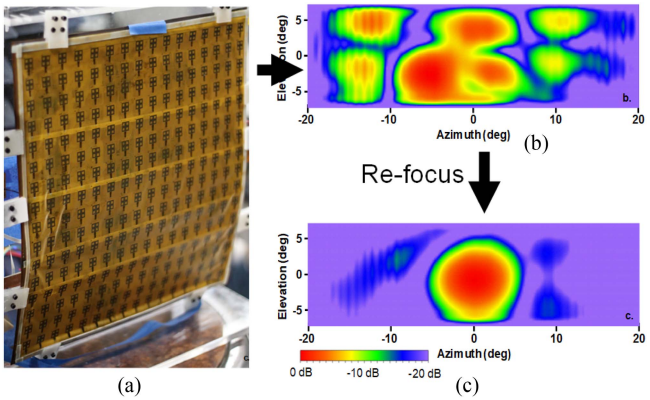

FIGURE 12. A 256-elements tile based array with deformation correction capabilities [82]. (a) 256-elements tile based array with deformed surface. (b) 2-D radiation patters with flat phase settings. (c) Post refocusing radiation pattern. Reprinted with permission.

Flexible phased array transmitters face an inherent thermal management challenge. The RFICs dissipate power and create heat which must be removed but the thin, light, flexible substrates generally have low thermal mass and thermal conductivity. The 256 element arrays shown in [70] use flexible copper strips as heatsinks attached to the back of the RFICs and convection for cooling. These copper strips are connected to the RFIC with thermal paste and attached to the flexible substrate with epoxy. This solution is suitable for terrestrial applications but can not be used for systems at high altitude or in space. Space-borne systems could use high emissivity surfaces to cool the RFICs. The development of flexible, mechanically robust, and efficient thermal management solutions would be boon to future shape-changing phased arrays.

C. EMERGING TECHNOLOGIES

Future flexible arrays stand to benefit from a range of research into flexible and non-flexible materials and systems that is not specifically intended for use in flexible arrays.

While the polyimide substrates used in many of the previously described works are flexible, they are not stretchable. A fully integrated stretchable phased array is yet to be published, but a variety of other stretchable electronic systems and components have been created. Elastomer substrates have emerged as a compelling candidate for stretchable electronic systems. An implantable system for neurostimulation with a stretchable multi-band microwave antenna was presented in [86]. A multi-layer elastomer circuit for human-machine interface applications was demonstrated in [87]. While these works use meandered lines to enable stretchability, stretchable conductive materials are also an active area of research. Liquid metals suspensions [88] and hydrogels [89] hold promise for future phased arrays. While the RF properties of these stretchable conductors are mostly unexplored, stretchable liquid metal antennas and a stretchable liquid metal mechanical phase shifter are shown in [90], [91].

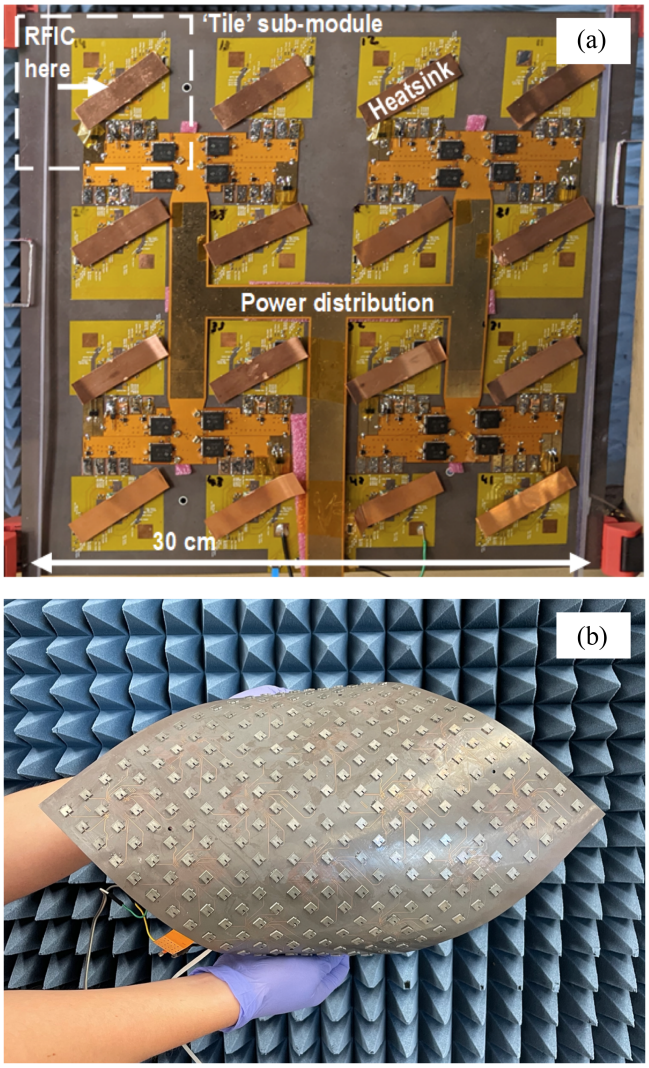

FIGURE 13. **An example of a modular, flexible tile-based array [70]. This example is made by repeating a 4 × 4 radiator unit cell driven by a single RFIC 16 times to create a 16 × 16 array of 256 radiators and 16 RFICs. (a) The back of the array, showing the individual unit cells, heatsinks to the RFICs, and the power distribution network. Licensed under CC BY 4.0. (b) The array, front-facing, bent along the diagonal.**

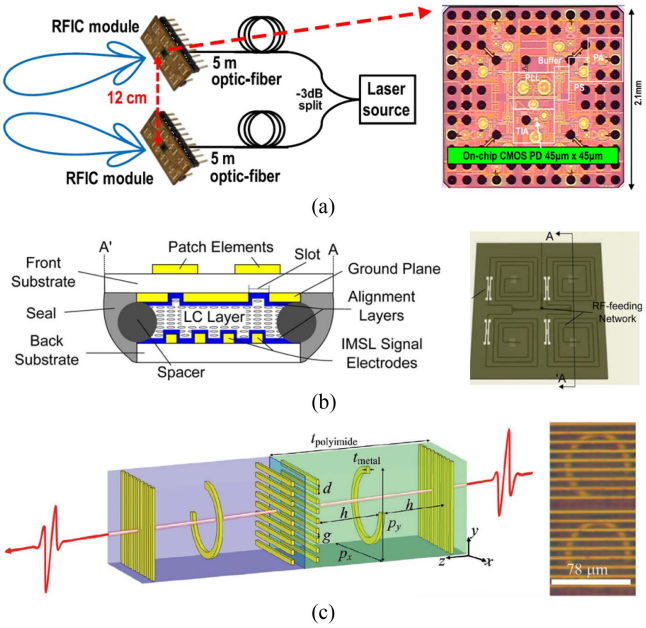

FIGURE 14. **Emerging flexible phased array technologies. (a) Optical timing synchronization [83] licensed under CC BY 4.0, (b) LCD based phased array [84] reprinted with permission, (c) metasurface THz phase shifter [85] licensed under CC BY 4.0.**

Distribution of clock and data signals for arrays with many elements is challenging for both rigid and flexible systems. Conventional distribution networks are difficult to scale without risking high loss, interference or unintentional radiation, and physical routing obstructions. A promising approach, shown in Fig. 14(a), aims to distribute these signals using an optical fiber to receivers that utilize bulk-integrated photodiodes to maintain overall simplicity [83].

Another potential tool for future flexible arrays is the utilization of LCD panels as antenna substrates. This enables the local control of LCD domains to manipulate phase accumulation as signals are routed to the different radiators [92], [93], as shown in Fig. 14(b) [84]. While LCD panels are not yet fully flexible, folding displays have already been demonstrated in smartphones and tablets. At higher frequencies (e.g., THz range), the flexible substrate itself is thick enough compared to the radiated wavelength that it is possible to synthesize meta-materials using various patterns etched onto the laminate metallization layer [85], as illustrated in Fig. 14(c). In [94], the authors demonstrate a meta-surface pattern loaded with a liquid crystal that together constitute a tunable meta-surface antenna.

While RFIC-based flexible arrays work to make traditional high performance systems mechanically compatible with bending, an alternative approach is to raise the performance of already flexible thin film transistors (TFTs). [98] is a 1x4 array built on a flexible substrate with TFT phase shifters. This work, as well as [75], are electronically steered flexible arrays but lack signal synthesis or element drive circuitry and must be driven by a signal generated and amplified by external circuitry. Alternatively, [95] presents a phased array in which both the phase shifters and RF power generation are based on TFTs. This work shows that an increase in the TFTs' frequency of operation beyond 1 GHz was possible through minimization of the parasitic capacitance that usually limits the operating frequency to the MHz-range. The array itself is composed of three TFT injection-locked oscillators, shown in Fig. 15(a) that are embedded in a larger rigid system to perform beam steering. Future incorporation of these TFT circuits into multi-functional flexible phased arrays either alone or in conjunction with higher RF performance, traditional process ICs is conceivable.

In [96], the authors demonstrate screen printing of vanadium dioxide (VO_2) switches, which are compatible with the large-scale fabrication of flexible RF electronics design.

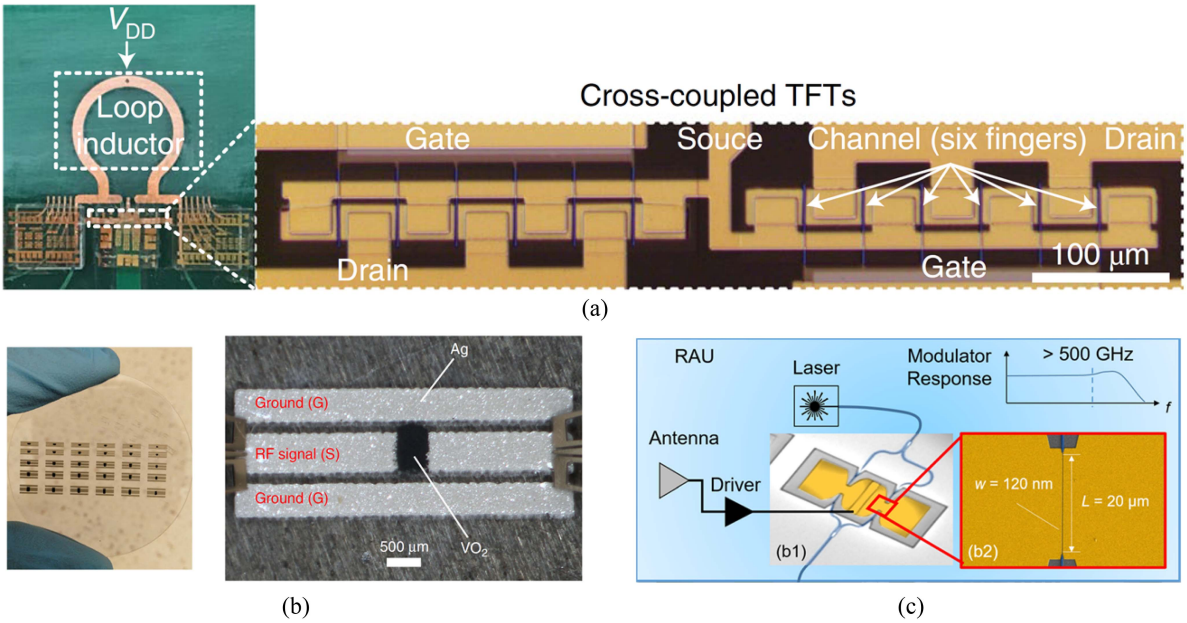

FIGURE 15. Emerging flexible phased array devices. (a) Thin film transistors [95] reprinted with permission, (b) RF switches [96] licensed under CC BY 4.0, and (c) opto-electornic modulators [97] licensed under CC BY 4.0.

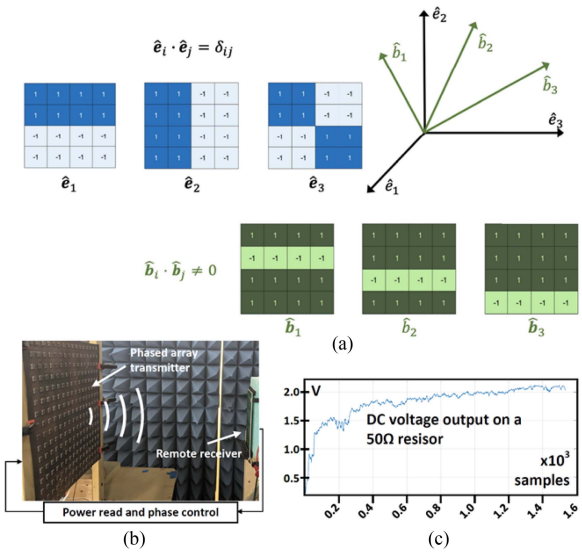

FIGURE 16. Refocusing of large arrays using a dynamic search algorithm, over groups of radiators that form an orthogonal basis for search over phase-space. (a) Example of Linearly independent, but non-orthogonal partial (three out of 16) mask-set (b_1, b_2, and b_3) and orthogonal partial (three out of 16) mask-set (e_1, e_2, and e_3) [41]. (b) Hardware used for execution of dynamic refocusing algorithm includes the antenna under test, a receiver with power measurement capability, and a feedback path to a computing device. (c) Example of refocusing a flexible antenna to a receiver rectenna terminated with 50 Ω load at 1 m away from the antenna plane. Reprinted with permission from [70].

The switches, shown in Fig. 15(b) were used to design a frequency-variable filter on a flexible substrate. One challenge for these switches is that the ON/OFF state is controlled by a variation of local temperature, in this case between 25 °C and 90 °C, which might limit the switching frequency and therefore the applications of this technology. The design of a 500 GHz optical-electronic modulator is demonstrated in [97]. The modulator shown in Fig. 15(c) is essentially a slot wave-guide, filled with a non-linear organic material. The dielectric constant of the organic material depends on the applied electric field, and thus, light passing through it can be modulated if an RF signal is simultaneously applied to the wave-guide. While this specific demonstration is not aimed at flexible RF/optical applications, the technology is compatible with flexible circuit materials and can be useful in a broad range of applications.

IV. SHAPE-CHANGING ARRAY OPERATION ALGORITHMS

Shape-changing arrays require a new paradigm of operation methods and calibration techniques that need to be developed. In this section, we discuss some of the approaches to handle these challenges.

A. FOCUSING AND REFOCUSING

One major operational challenge for a shape-changing phased array is the loss of radiator position information needed to determine phase settings for beamforming and focusing. With a rigid array, the element positions are static and the fixed phase offsets needed for beamforming and focusing are easily determined. However, the dynamic changes undergone by a shape-changing array can confound wavefront engineering if not properly addressed. One possible approach is to use the information from the intended receivers themselves to provide feedback to the transmit array about the quality of the beamforming or focusing. This information can be used by the transmit array to optimize the electromagnetic wavefront

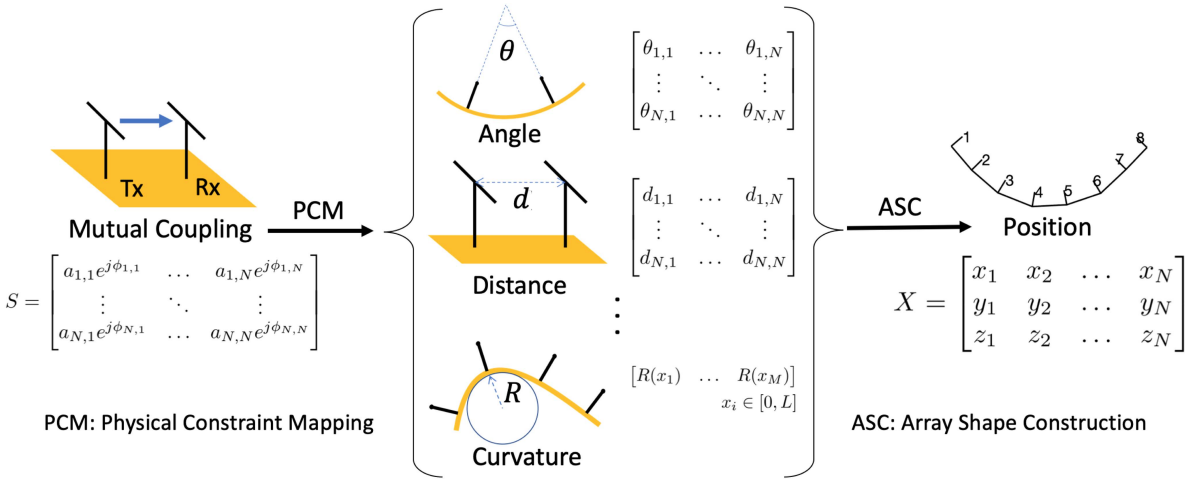

FIGURE 17. **A block diagram showing the two-step modular shape reconstruction approach. This figure was originally published in [68] and is licensed under CC BY-NC-ND 4.0.**

TABLE 1. **Shape-Changing Array Metrics**

	[72]	[71]	[68]	[49]	[70]	[44]	[43]	Target Space Array[a]	Target Deployable Array	Target Wearable Array
Frequency (GHz)	2.5	5	10	17-27	10	28	19	Any	Any	Any
Size (Elements)	5x5	4x4	1x8	22	16x16	4x8	32	~0.05 – 1 m^2 ~1 – 1000 m^2	~1 m^2	~0.01 m^2
Element Pitch (λ)	0.585	0.5	0.6	6[b]	0.6	<1[c]	Unknown	<1	<1	<1
EIRP (dBm)	30.5	No amplifiers	28[d]	No amplifiers	60.5	Unknown	RX with 16 dBi gain[e]	High Very High	Medium	Low
Phase Resolution (°)	<1	180	<2	No Phase Control	<2	<1	<1	<1	<1	<10
Shape-change Mechanism	Panelized origami	Flex substrate	Flex substrate	Panelized origami	Flex substrate	Flex substrate	Flex substrate	Any	Any	Any
Areal Mass (kg/m^2)	16.7[f]	Unknown	0.8	Unknown	1.06[f]	Unknown	Unknown	<0.3	<5	<1
Thickness (cm) [λ][g]	8 [0.7]	Unknown	0.9 [0.3]	Unknown	S: 0.1 [0.033] D: 0.4 [0.133][h]	0.03 [0.028][i]	0.05 [0.031][j]	<1	<5	<1
Min Bend Rad. (cm) [Norm][k]	10.25 [0.32]	Unknown	10 [0.61]	10 [0.25]	23 [0.72][l]	Unknown	Unknown	As needed to stow and deploy	[<1/π][m]	[<1/π][m]
Stretch Factor[n]	1	1	1	3	1	1	1	1	>2	>2
Shape Self-Measurement	No	No	Yes[o]	No	No	No	No	Yes	Yes	Yes
Convenient Interface?	Yes	No	No	No	Yes	No	No	Yes	Yes	Yes
Integration Level[p]	Ra,Ph,A,Dig.	Ra, Ph.	Ra,Ph,A,Dig.	Ra.	Ra,Ph,A,Dig.	Ra,Ph,A,Dig.	Ra,Ph,A,Dig.	Ra,Ph,A,Dig.	Ra,Ph,A,Dig.	Ra,Ph,A,Dig.

a. Space array could be used for communications or power transfer, as such some entries are split. **b.** Estimated from figure showing dense flat configuration using 22 GHz as operation frequency. **c.** Upper bound estimated from figures. **d.** Estimated from simulation. **e.** This is a receive array not a transmitter. **f.** Includes additional mass of interface cabling, heat spreaders, and support frames. **g.** [x] provides the thickness in units of the operating wavelength. **h.** Stowed and deployed configurations. **i.** Flexible circuit board thickness not including RFICs or interface connectors. **j.** Believed to be flexible circuit board thickness not including interface connectors. **k.** [x] is the bend radius normalized by the longest side of the array aperture **l.** Estimated from figure showing the Waterbomb origami surface in cylindrical configuration. **m.** A ratio for bend radius/aperture length of 1/π corresponds to an exact half cylinder bend. **n.** Defined as the largest achievable planar area over the smallest achievable planar area. **o.** Mutual coupling shape reconstruction. **p.** Are Radiators, Phase Shifters, Amplifiers, and Digital circuits present on the shape-changing array?

generated by controlling the phase and amplitude of the element excitations in response to mechanical variations of the array that happen on a much slower timescale.

However, such an approach faces challenges such as limited observable variations in the receiver signal due to small changes in a small number of elements - namely, a small dynamic range. Changing a single element can result in variations below the noise and drift of the received signal. Also, the potentially long propagation latency between the receiver and transmitter can significantly slow down the response of the system. Additionally, non-linearities in phase setting (due to, for example, frequency synthesizer pulling) present challenges that make it difficult to leverage existing optimization methods, many of which work best on linear systems.

'Focusing,' as presented in [41], is a generalization of far-field beam-forming that allows for the steering of a beam to a receiver at an arbitrary distance from the array using N-dimensional search techniques. One solution to clear a path through these variegated challenges is to utilize a novel batch search algorithm based on an orthogonal basis. One such

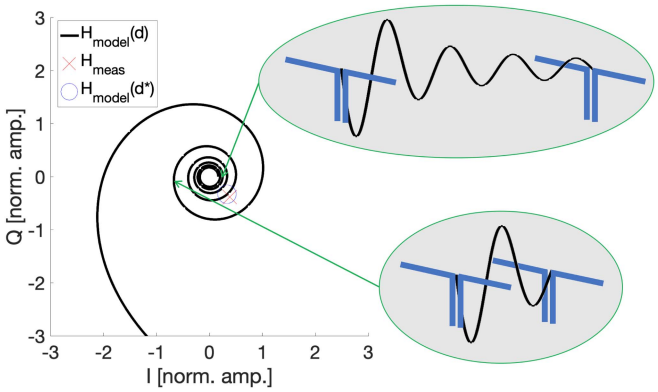

FIGURE 18. A Spiral Match projection. A model for the mutual coupling change, $H_{model}(d)$, is plotted in the complex (I/Q) plane. The measured coupling is mapped in the complex plane and projected onto the closest location on the model, $d*$. The spiral shape derives from linear phase progression but decreasing amplitude with distance, as shown with the two coupling pairs on the right. Each coupling pair distance is a single location on $H_{model}(d)$.

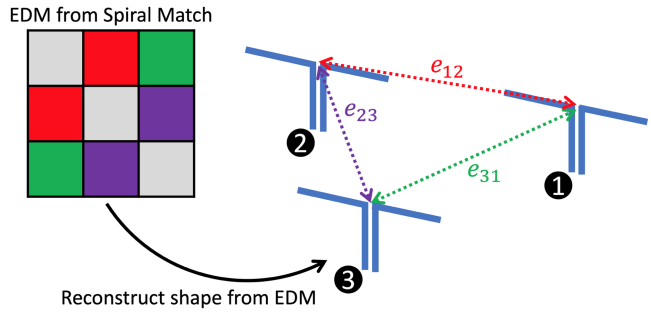

FIGURE 19. The process of multidimensional scaling (MDS). On the left: An EDM from the first step of the algorithm. On the right: the reconstructed shape.

example was originally presented in [41], which alters phases in orthogonal groups (determined, e.g, using Hadamard matrices, Fig. 16(a)) of radiators. This has the benefit of making enough change at once to trigger detectable changes in received power, while taking the full rank of the array into account.

Larger size bases enable phases of multiple elements to be varied simultaneously to achieve a much higher dynamic range. Furthermore, the use of orthogonal, or even pseudo-orthogonal bases allows a large number of different states to be batch generated and processed, to overcome the large latency issue. This batch processing algorithm does not have to wait for the result of the previous step to process the next and can evaluate and calculate the effect of a large number of variations all at once, thanks to the orthogonality. Finally, the orthogonal bases combined with the variable step approach are much more robust to non-linear variations in the system.

In the early iterations, searches are conducted over large spaces (a wide range of possible phases.) As the optimization proceeds, the search space is successively reduced by a scaling factor. This method has demonstrated success in various contexts and has successfully optimized large arrays with a proportionally low number of iterations (1000-2000 steps for a 256 element array.) The implementation of this algorithm involves detection of the power strength by the receiver (Fig. 16(b)). A microcontroller chip is programmed to run the optimization scheme and to use the signal strength as feedback. The motherboard then adjusts phases accordingly and communicates changes down to the daughter boards until maximum power is delivered to the receiver (Fig. 16(c)).

B. SHAPE RECONSTRUCTION

Although the closed loop feedback focusing approach provides an immediate and direct solution to overcome many of the challenges associated with the dynamically shape-changing arrays, it still presents limitations of its own. For instance, it relies on the existence of a receiver as well as a feedback communication channel. Either of these could be absent in certain applications.

To bypass some of these issues, the position of the elements in a shape-changing array can be found and then accounted for locally. This shape calibration can be performed with additional external sensors built onto the array surface such as [99]. In [100], a flexible inkjet printed bend sensor is shown which can sense bends in two axis and is intended for use in flexible phased array applications. These external sensor approaches give accurate local bend measurements but add additional hardware and may lack the higher dimensionality or global measurements needed for highly complex shapes.

Alternatively, [68], [101] propose and demonstrate a technique for reconstructing the shape of an array using only the array's mutual coupling and no additional external hardware, reusing already existing receiving and transmitting circuitry in the array. The reconstructed shape can then be used to determine the needed excitation phase for each element. Not only is this approach desirable for phase correction on shape-changing arrays, but it also opens up the doors to new applications. Instead of using the array for power transfer or communication, the shape reconstruction can be a means unto itself - potentially useful as a sensor, or a combined sensor and communication link for a various applications ranging from virtual reality interfaces to building and structures shape monitoring.

The shape reconstruction method uses a two-step approach. The first step maps the mutual coupling measurements performed by the RFICs to a physical parameter, such as the distance of the elements relative to one another. The second step uses the estimated physical parameters (e.g., distance between pairs) to construct the shape of the shape changing array.

This method, shown graphically in Fig. 17, relies on the use of a physical parameter, be it local curvature, distance, angle, etc. to serve as an intermediary between the mutual coupling and the relative shape. These implementations of the two-step modular approach utilize distance between one antenna and another (the Euclidean distance) because of the simplicity of propagation models mapping coupling to distance and algorithms that map distance to shape.

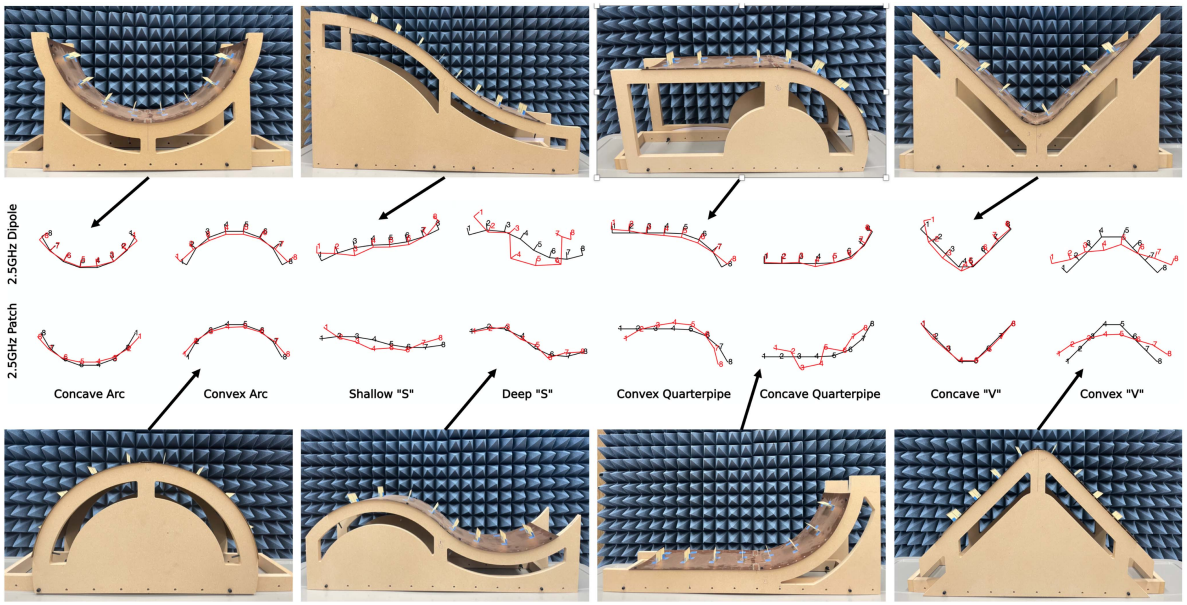

FIGURE 20. Middle: The side view of various 1D symmetric and asymmetric shapes reconstructed from mutual coupling matrices collected from flexible, passive 8 × 1 arrays using the two-step modular approach. The ground truth is in black while the reconstructed shape is shown in red. Number denote element indices. The results presented are for both patch and dipole arrays. Top and bottom: images of the shapes with dipole array installed, chosen instead of patch array photos because the dipole antennas are more visible at this side angle.

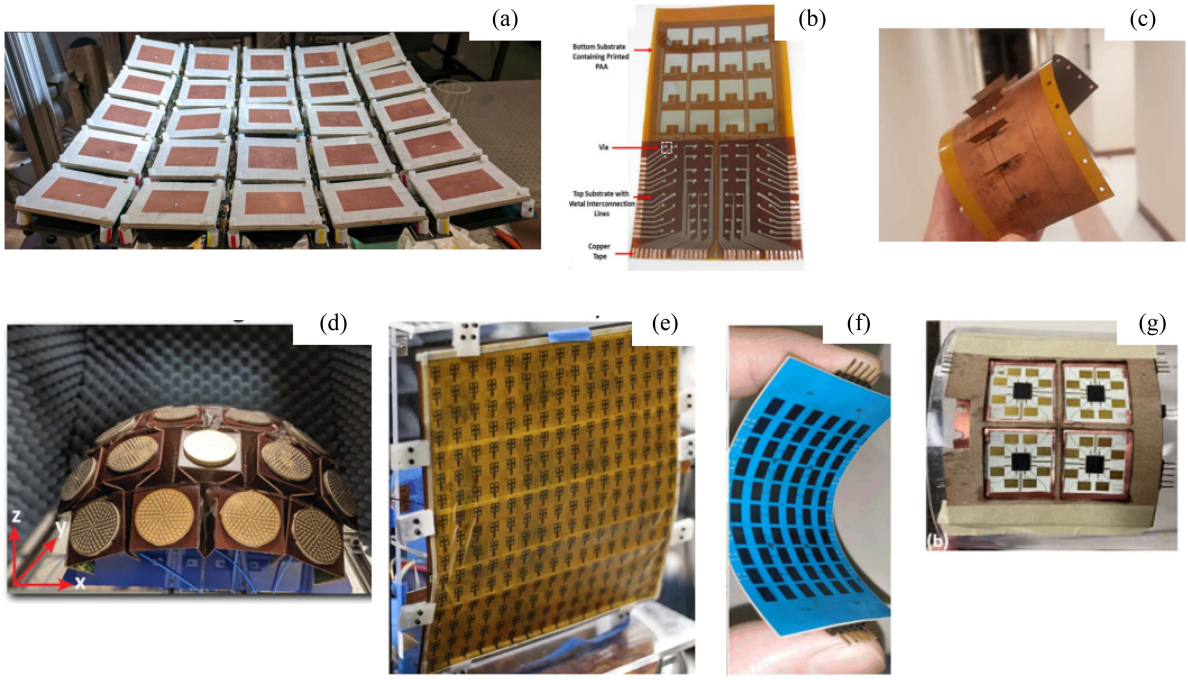

FIGURE 21. Arrays found in Table 1. (a) [72], reproduced with permission. (b) [71], reproduced with permission. (c) [68], licensed by CC BY-NC-ND 4.0. (d) [49], licensed by CC BY 4.0 (e) [70], licensed by CC BY 4.0. (f) [44], reproduced with permission. (g) [43], reproduced with permission.

The following model, inspired by the Friis model for free-space propagation, is used to map mutual coupling (S_{mn}) to Euclidean distance, as below:

$$S_{mn} = \frac{a_m D_m(\theta_{mn}, \phi_{mn}) a_j D_n(\theta_{nm}, \phi_{nm})}{|\vec{l_{mn}}|} e^{-j(\phi_m + \phi_n + k|\vec{l_{mn}}|)} \quad (1)$$

where a_m is the total fixed amplitude offset (due to line attenuation, mismatch, gain, etc.) in antenna m, $D_m(\theta, \phi)$ is the directivity of antenna m for angles θ and ϕ relative to broadside, $\vec{l_{mn}}$ is the vector pointing from the phase center of antenna i to the phase center of antenna n, $|\vec{l_{mn}}|$ is the Euclidean distance, and ϕ_m is the total fixed phase offset in antenna m. This coupling expression is the heart of "Spiral

Match" which maps coupling to physical distance. As shown in Fig. 18, the namesake spiral emerges from decreasing amplitude and rotating phase as distance, $|\vec{l_{mn}}|$, increases. A normalization by the flat configuration to remove offsets and an iterative projection of the measured coupling value onto the physically realizable couplings described by the spiral are needed before a matrix of distance pairs is created.

The assembled distance pairs are called a Euclidean Distance Matrix (EDM). With the EDM the first step of the approach ends and the second - translating the distances to shape - begins. This is accomplished using algorithms originally conceived of by the signal processing community which make use of multidimensional scaling (MDS). MDS takes in an EDM, "centers" it geometrically, and performs an eigenvalue decomposition on the centered matrix. A multiplication of the first d (where d is the number of dimensions the shape is expected to live in) eigenvalues by the first d eigenvectors gives us the relative shape matrix. This method has found use in numerous applications including but not limited to predicting molecular configurations from inter-atomic distances, calibrating the microphones and speakers in a theatre, mapping nodes on a network, and protein shape prediction. The EDM-relative shape concept is shown in Fig. 19. There are variety of MDS implementation methods. Based on the analysis in [102], semi-definite-relaxation (SDR) is the best candidate for noisy but complete matrices such as are present in the context of shape reconstruction for phased arrays.

SDR was used on EDMs created by Spiral Match for mutual coupling matrics collected from connectorized arrays bent to various constant curvatures in [68]. For these 2.5 GHz passive arrays, one with patch antennas and another with dipoles, error ranged from 3% to 7% of λ. On a 10 GHz active array driven by the custom transceiver RFIC presented in the same work error ranged from 3% to 11% of λ.

The previously presented Spiral Match algorithmn used a local constant curvature assumption. The constant curvature assumption is used locally for coupling pairs but not globally for the entire shape - shape reconstruction through MDS allows for the prediction of irregular shapes. However, removing the assumption of constant curvature from the algorithm entirely can enhance the probability that distances derived from an asymmetric shape are predicted accurately. This work presents a new method for shape reconstruction that does not use the constant curvature assumption. The assumption was used in [68] as a simple means of mapping coupling angles and distances; this mapping is, however, unnecessary. If we search over angles and distances independently, the assumption of constant curvature can be dropped.

This higher dimensional search requires few modifications to the algorithm. The previous implementation iterated over l_{mn} in Spiral Match, instead the new algorithm iterates over tuples of $(l_{mn}, \theta_{mn}, \theta_{nm})$[1]. This makes the search space larger and increases the associated runtime and algorithmic complexity, but allows for better prediction of asymmetric shapes. Indeed, the method using a high-dimensional search space achieves a mean position error of 18% of λ when stressed with irregular shapes (two sinusoids, two "quarter pipes," and a "V"), on dipoles and patches, as shown in Fig. 20.

This figure emphasizes the bimodal results that the reconstruction method produces. On the one hand, there are shapes, such as the concave arc, convex arc, concave "V," shallow "S," or convex quarterpipe, where the method predicts a shape in good agreement and low position error relative to the ground truth. On the other hand, we have the Deep "S" for dipoles or the Concave Quarterpipe for patches, where the the shape looks erratic, apparently violating fundamental physical constraints on the fixed distance between adjacent antennas. While the algorithm accurately reconstructs all tested constant curvature shapes and many shapes with asymmetric curvature, high position error can be caused by several factors. An error could arise (say from improperly handled phase wrapping, introducing errors of multiples of 2π) in the first step of the method which predicts distance from mutual coupling. This error result in highly non-physical EDM - usually only with respect to a few matrix entries. These "anomalous matrix entries" present a challenge for SDR which correctly identifies the matrix as non-physical but may not converge to an accurate correction when optimizing. If SDR does not converge to something accurate, it typically "seizes up" and converges to something that bears little resemblance to the initial EDM. Thus, the final relative shape looks erratic and the distances violate physical constraints even though most of the EDM entries did not.

These results present opportunities and challenges that can serve as a starting point for further lines of inquiry. It is conceivable to design a method which selectively excises EDM entries which appear incompatible with the others. Doing this would likely allow the SDR to converge to an accurate shape reconstruction. Furthermore, the electromagnetic model of mutual coupling used in the algorithm can be improved to capture the essence of the near-field coupling more accurately. For cases such as the Convex "V," it is unlikely that the simplified propagation model accurately captures coupling behavior when the elements line-of-sight views are heavily occluded. As an alternative, it is possible multi-frequency coupling measurements (shown in [103]), which add measurement diversity and remove phase ambiguity, could solve these issues without requiring a substantially more complex coupling model. These ideas and concepts present exciting paths toward the future of this class of shape reconstruction methods to be use in shape-changing arrays.

V. CONCLUSION

A. ASSESSING SHAPE-CHANGING ARRAYS

A diverse set of shape-changing arrays have been presented and described in this work. Table 1 compares several of these arrays across a broad range of metrics and capabilities. The arrays of Table 1 are shown in Fig. 21. Because the intended

[1]It can be shown that for shapes of non-constant curvature, θ_{mn} and θ_{nm} are not always the same, unlike the coupling distance l_{mn}, which obeys the symmetry principle: $l_{mn} = l_{nm}$.

use and functionality of these arrays varies widely, it is difficult to compare them with any single parameter. Stowablility, stretchability, ultra low mass, or self-shape calibration may be critically important or entirely unnecessary depending on the application.

The electrical interface and integration level metrics capture some of the logistical challenges of deploying these array implementations. The ideal electrical interface is minimally intrusive, such as a small ribbon of flat flexible cables interfacing over a narrow section of a single side of the shape-changing array as found in [70], [72]. Less optimally, [43], [44], [68] require cables or connectors on multiple edges of their flexible substrate. These cables and connectors constrain the array mechanically. [75] uses an entire side of the array to interface with its phase control units limiting scalability, and [49] requires an RF interface with each individual element. The arrays which are not fully integrated shape-changing arrays ([75] and [49]) also require additional external circuitry for their operation. This external circuitry and cabling brings added mass and rigidity which precludes some of the intended applications for shape-changing arrays. While these specific demonstrated arrays were not fully integrated, there is no fundamental barrier to integrating additional circuitry onto their demonstrated shape-changing components. For example, the Waterbomb origami surface and wideband metasurface radiators of [49] could be combined with multifunction, panelized electronics similar to [72].

In addition to realized prototypes, Table 1 includes three fictitious target shape-changing arrays. The characteristics for these targets were selected based the needs of three potential applications of shape-changing arrays. For a space deployable arrays (such as the space solar power arrays proposed in [45], [46] or the communication arrays of [43], [44]), low mass and high power are priorities while stretchability and bending are only needed to compactly store the system prior to deployment. A deployable terrestrial array serving as a rapid-response communication or sensing hub benefits from bending to create a horizon to horizon field-of-view but minimizing its low mass and thickness is less important. A wearable array must stretch and bend to properly conform to the human body but likely has less need for high power beams with precise phase control. The capability gap between the realized arrays and the target arrays highlights the substantial opportunities for innovation which exist for shape-changing arrays.

B. CHALLENGES, PROGRESS, AND OPPORTUNITIES

There are significant challenges which must be overcome in order to take the hypothetical target arrays from columns in Table 1 to physical prototypes on a lab-bench and in the field. Even with the advancements presented here, the principle challenges remain only partially met. Synchronizing element excitations with regard to phase offsets, position offsets, and orientation without at-target-feedback requires several techniques employed simultaneously in conjunction with mutual coupling shape-calibration. Maintaining flexibility while distributing DC power, digital control signals, frequency/phase reference information, and high bandwidth data to each element requires careful architecture and component electro-mechanical co-design. Thermal management will always be a concern for thin, low thermal mass and conductivity arrays using heat-concentrating RFICs. Mechanical reliablility over many deformation cycles, especially at solder joints, must also be carefully monitored for flexible or stretchable arrays. Finally, these issues must be solved with an eye towards scalability and manufacturability. Small-scale, artisanal, "one-off" designs characteristic of academic labs will not meet the operational or volume requirements of real applications.

While these challenges are considerable, in this paper we showed several families of shape-changing arrays, whose versatility, flexibility, and low-mass nature bring us closer to the vision of the asymptotic flexible array system that is as light and flexible as a sheet of paper. Thin, light, large-scale flexible arrays were shown in [82], mechanically reliable, deployable, and flex compatible radiators were demonstrated in [69], and a shape reconstruction technique for dealing with shape change was shown in [68], [101]. These and other works represent important steps toward the asymptotic system and are yet to reach their full potential. The combination of these components and capabilities on a single platform with IO and control suitable for a range of applications including communications, sensing, and power transfer will unlock the full potential of shape-changing phased arrays.

REFERENCES

[1] E. Jones and J. Shimizu, "A wide-band transverse-slot flush-mounted array," *IRE Trans. Antennas Propag.*, vol. 8, no. 4, pp. 401–407, Jul. 1960.

[2] W. Rotman and A. A. Oliner, "Periodic structures in trough waveguide," *IRE Trans. Microw. Theory Techn.*, vol. 7, no. 1, pp. 134–142, Jan. 1959.

[3] A. Ishimaru and H.-S. Tuan, "Frequency scanning antennas," in *Proc. 1958 IRE Int. Conv. Rec.*, 1961, vol. 9, pp. 101–109.

[4] J. Spradley, "A volumetric electrically scanned two-dimensional microwave antenna array," in *Proc. IRE Int. Conv. Rec.*, 1958, vol. 6, pp. 204–212.

[5] R. Roush and J. Wiltse, "Electronically steerable S-band array," *IRE Trans. Antennas Propag.*, vol. 9, no. 1, pp. 107–109, Jan. 1961.

[6] L. Stark, "Microwave theory of phased-array antennas–A review," *Proc. IEEE*, vol. 62, no. 12, pp. 1661–1701, Dec. 1974.

[7] C. Donn and A. E. Bollesen, "A 16-element, K-band monolithic active receive phased array antenna," in *Proc. IEEE AP-S. Int. Symp., Antennas Propag.*, 1988, vol. 1 pp. 188–191.

[8] J. Potukuchi, R. Mott, A. Zaghloul, R. Gupta, F. Assal, and R. Sorbello, "MMICs insertion in a ku-band active phased array for communications satellites," in *IEEE Int. Dig. Microw. Symp.*, vol. 2, pp. 881–884, 1990.

[9] W. Hong et al., "The role of millimeter-wave technologies in 5G/6G wireless communications," *IEEE J. Microwaves*, vol. 1, no. 1, pp. 101–122, Jan. 2021.

[10] H. Wu and A. Hajimiri, "A 10 GHz CMOS distributed voltage controlled oscillator," in *Proc. IEEE Custom Integr. Circuits Conf.*, 2000, pp. 581–584.

[11] H. Wu and A. Hajimiri, "A 19 GHz 0.5 mW 0.35/spl mu/m CMOS frequency divider with shunt-peaking locking-range enhancement," in *Int. Solid-State Circuits Conf. Dig. Tech. Papers*, 2001, pp. 412–413.

[12] X. Guan and A. Hajimiri, "A 24 GHz CMOS front-end," in *Proc. 28th Eur. Solid-State Circuits Conf.*, 2002, pp. 155–158.

[13] X. Guan and A. Hajimiri, "A 24-GHz CMOS front-end," *IEEE J. Solid-State Circuits*, vol. 39, no. 2, pp. 368–373, Feb. 2004.

[14] X. Guan, H. Hashemi, and A. Hajimiri, "A fully integrated 24-GHz eight-element phased-array receiver in silicon," *IEEE J. Solid-State Circuits*, vol. 39, no. 12, pp. 2311–2320, Dec. 2004.

[15] A. Hajimiri, A. Komijani, A. Natarajan, R. Chunara, X. Guan, and H. Hashemi, "Phased array systems in silicon," *IEEE Commun. Mag.*, vol. 42, no. 8, pp. 122–130, Aug. 2004.

[16] H. Hashemi, X. Guan, A. Komijani, and A. Hajimiri, "A 24-GHz SiGE phased-array receiver-LO phase-shifting approach," *IEEE Trans. Microw. Theory Techn.*, vol. 53, no. 2, pp. 614–626, Feb. 2005.

[17] A. Hajimiri, H. Hashemi, A. Natarajan, X. Guan, and A. Komijani, "Integrated phased array systems in silicon," *Proc. IEEE*, vol. 93, no. 9, pp. 1637–1655, Sep. 2005.

[18] A. Natarajan, A. Komijani, and A. Hajimiri, "A fully integrated 24-GHz phased-array transmitter in CMOS," *IEEE J. Solid-State Circuits*, vol. 40, no. 12, pp. 2502–2514, Dec. 2005.

[19] A. Komijani, A. Natarajan, and A. Hajimiri, "A 24-GHz, 14.5-dBm fully integrated power amplifier in 0.18-/spl mu/m CMOS," *IEEE J. Solid-State Circuits*, vol. 40, no. 9, pp. 1901–1908, Sep. 2005.

[20] C. H. Doan, S. Emami, A. M. Niknejad, and R. W. Brodersen, "Millimeter-wave CMOS design," *IEEE J. Solid-State Circuits*, vol. 40, no. 1, pp. 144–155, Jan. 2005.

[21] C. Marcu et al., "A 90 nm CMOS low-power 60 GHz transceiver with integrated baseband circuitry," *IEEE J. Solid-State Circuits*, vol. 44, no. 12, pp. 3434–3447, Dec. 2009.

[22] A. Babakhani, X. Guan, A. Komijani, A. Natarajan, and A. Hajimiri, "A 77-GHz phased-array transceiver with on-chip antennas in silicon: Receiver and antennas," *IEEE J. Solid-State Circuits*, vol. 41, no. 12, pp. 2795–2806, Dec. 2006.

[23] A. Natarajan, A. Komijani, X. Guan, A. Babakhani, and A. Hajimiri, "A 77-GHz phased-array transceiver with on-chip antennas in silicon: Transmitter and local LO-path phase shifting," *IEEE J. Solid-State Circuits*, vol. 41, no. 12, pp. 2807–2819, Dec. 2006.

[24] B.-W. Min and G. M. Rebeiz, "Single-ended and differential Ka-band BiCMOS phased array front-ends," *IEEE J. Solid-State Circuits*, vol. 43, no. 10, pp. 2239–2250, Oct. 2008.

[25] D.-W. Kang, J.-G. Kim, B.-W. Min, and G. M. Rebeiz, "Single and four-element *ka*-band transmit/receive phased-array silicon RFICs with 5-bit amplitude and phase control," *IEEE Trans. Microw. Theory Techn.*, vol. 57, no. 12, pp. 3534–3543, Dec. 2009.

[26] S. Jeon et al., "A scalable 6-to-18 GHz concurrent dual-band quad-beam phased-array receiver in CMOS," *IEEE J. Solid-State Circuits*, vol. 43, no. 12, pp. 2660–2673, Dec. 2008.

[27] A. Valdes-Garcia et al., "A fully integrated 16-element phased-array transmitter in SiGe BiCMOS for 60-GHz communications," *IEEE J. Solid-State Circuits*, vol. 45, no. 12, pp. 2757–2773, Dec. 2010.

[28] S. Emami et al., "A 60 GHz CMOS phased-array transceiver pair for multi-Gb/s wireless communications," in *Proc. IEEE Int. Solid-State Circuits Conf.*, 2011, pp. 164–166.

[29] A. Natarajan et al., "A fully-integrated 16-element phased-array receiver in SiGe BiCMOS for 60-GHz communications," *IEEE J. Solid-State Circuits*, vol. 46, no. 5, pp. 1059–1075, May 2011.

[30] S. S. Ahmed, A. Schiessl, and L.-P. Schmidt, "Multistatic mm-wave imaging with planar 2d-arrays," in *Proc. German Microw. Conf.*, 2009, pp. 1–4.

[31] S. S. Ahmed, A. Schiessl, and L.-P. Schmidt, "Novel fully electronic active real-time millimeter-wave imaging system based on a planar multistatic sparse array," in *Proc. IEEE MTT-S Int. Microw. Symp.*, 2011, pp. 1–4.

[32] B. Sadhu et al., "A 28-GHz 32-element TRX phased-array IC with concurrent dual-polarized operation and orthogonal phase and gain control for 5G communications," *IEEE J. Solid-State Circuits*, vol. 52, no. 12, pp. 3373–3391, Dec. 2017.

[33] K. K. W. Low, S. Zihir, T. Kanar, and G. M. Rebeiz, "A 27–31-GHz 1024-element Ka-band SATCOM phased-array transmitter with 49.5-dBW peak EIRP, 1-dB AR, and ±70° beam scanning," *IEEE Trans. Microw. Theory Techn.*, vol. 70, no. 3, pp. 1757–1768, Mar. 2022.

[34] N. M. Monroe, G. C. Dogiamis, R. Stingel, P. Myers, X. Chen, and R. Han, "Electronic THz pencil beam forming and 2D steering for high angular-resolution operation: A 98 × 98-unit 265 GHz CMOS reflectarray with in-unit digital beam shaping and squint correction," in *Proc. IEEE Int. Solid- State Circuits Conf.*, 2022, vol. 65, pp. 1–3.

[35] J. Sun, E. Timurdogan, A. Yaacobi, E. S. Hosseini, and M. R. Watts, "Large-scale nanophotonic phased array," *Nature*, vol. 493, pp. 195–299, Jan. 2013. [Online]. Available: https://doi.org/10.1038/nature11727

[36] B. Abiri, F. Aflatouni, A. Rekhi, and A. Hajimiri, "Electronic two-dimensional beam steering for integrated optical phased arrays," in *Proc. Opt. Fiber Commun. Conf.*, 2014, Art. no. M2K.7. [Online]. Available: https://opg.optica.org/abstract.cfm?URI=OFC-2014-M2K.7

[37] R. Fatemi, B. Abiri, A. Khachaturian, and A. Hajimiri, "High sensitivity active flat optics optical phased array receiver with a two-dimensional aperture," *Opt. Exp.*, vol. 26, no. 23, pp. 29983–29999, Nov. 2018, doi: 10.1364/OE.26.029983. [Online]. Available: https://www.opticsexpress.org/abstract.cfm?URI=oe-26-23-29983

[38] K. Sengupta, D. Seo, L. Yang, and A. Hajimiri, "Silicon integrated 280 GHz imaging chipset with 4× 4 SiGe receiver array and CMOS source," *IEEE Trans. THz Sci. Technol.*, vol. 5, no. 3, pp. 427–437, May 2015.

[39] Y. Tousi and E. Afshari, "14.6 A scalable THz 2D phased array with 17 dBm of EIRP at 338 GHz in 65nm bulk CMOS," in *IEEE Int. Solid-State Circuits Conf. Dig. Tech. Papers*, 2014, pp. 258–259.

[40] R. Han and E. Afshari, "A CMOS high-power broadband 260-GHz radiator array for spectroscopy," *IEEE J. Solid-State Circuits*, vol. 48, no. 12, pp. 3090–3104, Dec. 2013.

[41] A. Hajimiri, B. Abiri, F. Bohn, M. Gal-Katziri, and M. H. Manohara, "Dynamic focusing of large arrays for wireless power transfer and beyond," *IEEE J. Solid-State Circuits*, vol. 56, no. 7, pp. 2077–2101, Jul. 2021.

[42] B.-H. Ku, O. Inac, M. Chang, and G. M. Rebeiz, "75–85 GHz flip-chip phased array RFIC with simultaneous 8-transmit and 8-receive paths for automotive radar applications," in *Proc. IEEE Radio Freq. Integr. Circuits Symp.*, 2013, pp. 371–374.

[43] K. Hu, G. Soto–Valle, Y. Cui, and M. M. Tentzeris, "Flexible and scalable additively manufactured tile-based phased arrays for satellite communication and 50 mm wave applications," in *Proc. IEEE/MTT-S Int. Microw. Symp.*, 2022, pp. 691–694.

[44] X. Wang et al., "A flexible implementation of Ka-band active phased array for satellite communication," in *Proc. IEEE/MTT-S Int. Microwave Symp.*, 2022, pp. 753–756.

[45] C. T. Rodenbeck et al., "Microwave and millimeter wave power beaming," *IEEE J. Microwaves*, vol. 1, no. 1, pp. 229–259, Jan. 2021.

[46] A. Fikes et al., "The Caltech space solar power project: Design, progress, and future direction," in *Proc. IEEE WiSEE Space Sol. Power Workshop*, 2022.

[47] M. R. M. Hashemi et al., "A flexible phased array system with low areal mass density," *Nature Electron.*, vol. 2, no. 5, pp. 195–205, May 2019. [Online]. Available: https://doi.org/10.1038/s41928-019-0247-9

[48] S. Zhang et al., "Standalone stretchable RF systems based on asymmetric 3D microstrip antennas with on-body wireless communication and energy harvesting," *Nano Energy*, vol. 96, 2022, Art. no. 107069. [Online]. Available: https://www.sciencedirect.com/science/article/pii/S2211285522001525

[49] S. Venkatesh, D. Sturm, X. Lu, R. J. Lang, and K. Sengupta, "Origami microwave imaging array: Metasurface tiles on a shape-morphing surface for reconfigurable computational imaging," *Adv. Sci.*, vol. 9, no. 28, 2022, Art. no. 2105016. [Online]. Available: https://onlinelibrary.wiley.com/doi/abs/10.1002/advs.202105016

[50] M. Kobayashi, C.-K. Jen, and D. Levesque, "Flexible ultrasonic transducers," *IEEE Trans. Ultrason., Ferroelect., Freq. Control*, vol. 53, no. 8, pp. 1478–1486, Aug. 2006.

[51] R. S. Singh et al., "P3D-6 simulation, fabrication, and characterization of a novel flexible, conformal ultrasound transducer array," in *Proc. IEEE Ultrason. Symp.*, 2007, pp. 1824–1827.

[52] M. Kobayashi, C.-K. Jen, and D. Levesque, "Flexible ultrasound transceiver array for non-invasive surface-conformable imaging enabled by geometric phase correction," *IEEE Trans. Ultrason., Ferroelectr., Freq. Control*, vol. 12, no. 16183, pp. 1–12, Sep. 2022.

[53] A. Pressley, *Elementary Differential Geometry*. London, U.K.: Springer, 2010. [Online]. Available: https://link.springer.com/10.1007/978-1-84882-891-97D

[54] R. J. Lang, *Twists, Tilings, and Tessellations: Mathematical Methods for Geometric Origami*. Boca Raton, FL, USA: CRC Press, 2017.

[55] X. He, Y. Cui, and M. M. Tentzeris, "Tile-based massively scalable MIMO and phased arrays for 5G/B5G-enabled smart skins and reconfigurable intelligent surfaces," *Sci. Rep.*, vol. 12, no. 1, Feb. 2022, Art. no. 2741. [Online]. Available: https://doi.org/10.1038/s41598-022-06096-9

[56] P.-S. Kildal, E. Martini, and S. Maci, "Degrees of freedom and maximum directivity of antennas: A bound on maximum directivity of nonsuperreactive antennas," *IEEE Antennas Propag. Mag.*, vol. 59, no. 4, pp. 16–25, Aug. 2017. [Online]. Available: https://ieeexplore.ieee.org/document/7954002/

[57] D. E. Williams, C. Dorn, S. Pellegrino, and A. Hajimiri, "Origami-inspired shape-changing phased array," in *Proc. IEEE 50th Eur. Microw. Conf.*, 2021, pp. 344–347.

[58] W. Liu, C. Zhu, and D. Wu, "Flexible and stretchable ultrasonic transducer array conformed to complex surfaces," *IEEE Electron Device Lett.*, vol. 42, no. 2, pp. 240–243, Feb. 2021.

[59] Z. Wu and T. Cui, "Shrink-induced microelectrode arrays for trace mercury ions detection," *IEEE Sensors J.*, vol. 19, no. 7, pp. 2435–2441, Apr. 2019.

[60] S. R. Seiler et al., "An origami inspired circularly-polarized folding patch antenna array," in *Proc. IEEE Int. Symp. Antennas Propag. USNC/URSI Nat. Radio Sci. Meeting*, 2018, pp. 181–182.

[61] I. Gupta and A. Ksienski, "Effect of mutual coupling on the performance of adaptive arrays," *IEEE Trans. Antennas Propag.*, vol. 31, no. 5, pp. 785–791, Sep. 1983.

[62] F. Jalili, D. E. Serup, O. Franek, M. Shen, and G. F. Pedersen, "Antenna array inter-element coupling impact on linearization of active phased array," in *Proc. IEEE Int. Symp. Netw., Comput. Commun.*, 2021, pp. 1–5.

[63] D. M. Pozar, "The active element pattern," *IEEE Trans. Antennas Propag.*, vol. 42, no. 8, pp. 1176–1178, Aug. 1994.

[64] Y. Li, A. Chandra, C. J. Dorn, and R. J. Lang, "Reconfigurable surfaces employing linear-rotational and bistable-translational (LRBT) joints," *Int. J. Solids Structures*, vol. 207, pp. 22–41, 2020. [Online]. Available: https://www.sciencedirect.com/science/article/pii/S0020768320303796

[65] D. E. Williams and A. Hajimiri, "Meta-gaps for mechanically reconfigurable phased arrays," in *Proc. IEEE 52nd Eur. Microw. Conf.*, 2022, pp. 656–659.

[66] K. Jawed, N. Kazem, and C. Majidi, "Soft-matter electronics and multifunctional materials with polydisperse liquid metal suspensions: Material architecture, principles, and applications to programmable matter," in *Proc. IEEE Int. Symp. Antennas Propag. USNC/URSI Nat. Radio Sci. Meeting*, 2017, pp. 417–418.

[67] H.-C. Teng, P.-J. Lin, M.-K. Chen, Y.-J. Huang, and S.-L. Fu, "Planar antennas on flexible substrate for wireless applications," in *Proc. Int. Conf. Electron. Mater. Packag.*, 2007, pp. 1–4.

[68] A. Fikes, O. S. Mizrahi, and A. Hajimiri, "A framework for array shape reconstruction through mutual coupling," *IEEE Trans. Microw. Theory Techn.*, vol. 69, no. 10, pp. 4422–4436, Oct. 2021.

[69] A. Fikes, O. S. Mizrahi, A. Truong, F. Wiesemüller, S. Pellegrino, and A. Hajimiri, "Fully collapsible lightweight dipole antennas," in *Proc. IEEE Int. Symp. Antennas Propag. USNC-URSI Radio Sci. Meeting*, 2021, pp. 545–546.

[70] M. Gal-Katziri, A. Fikes, and A. Hajimiri, "Flexible active antenna arrays," *npj Flex Electron.*, vol. 6, no. 1, pp. 1–11, Oct. 2022.

[71] J. G. D. Hester and M. M. Tentzeris, "Inkjet-printed flexible mm-wave Van-Atta reflectarrays: A solution for ultralong-range dense multitag and multisensing chipless RFID implementations for IoT smart skins," *IEEE Trans. Microw. Theory Techn.*, vol. 64, no. 12, pp. 4763–4773, Dec. 2016.

[72] D. E. Williams, C. Dorn, S. Pellegrino, and A. Hajimiri, "Origami-inspired shape-changing phased array," in *Proc. IEEE 50th Eur. Microw. Conf.*, 2021, pp. 344–347.

[73] A. C. Fikes, A. Safaripour, F. Bohn, B. Abiri, and A. Hajimiri, "Flexible, conformal phased arrays with dynamic array shape self-calibration," in *Proc. IEEE MTT-S Int. Microw. Symp.*, 2019, pp. 1458–1461.

[74] C. A. Balanis, *Antenna Theory: Analysis and Design*, 4th ed. Hoboken, NJ, USA: Wiley, Jan. 2016.

[75] H. Subbaraman et al., "Inkjet-printed two-dimensional phased-array antenna on a flexible substrate," *IEEE Antennas Wireless Propag. Lett.*, vol. 12, pp. 170–173, 2013.

[76] A. Eid, J. G. D. Hester, and M. M. Tentzeris, "5G as a wireless power grid," *Sci. Rep.*, vol. 11, no. 1, pp. 1–9, Jan. 2021. [Online]. Available: https://doi.org/10.1038/s41598-020-79500-x

[77] P. Lacomme, "New trends in airborne phased array radars," in *Proc. IEEE Int. Symp. Phased Array Syst. Technol.*, 2003, pp. 17–22.

[78] P. D. Hilario Re, S. K. Podilchak, S. A. Rotenberg, G. Goussetis, and J. Lee, "Circularly polarized retrodirective antenna array for wireless power transmission," *IEEE Trans. Antennas Propag.*, vol. 68, no. 4, pp. 2743–2752, Apr. 2020.

[79] E. Gdoutos et al., "A lightweight tile structure integrating photovoltaic conversion and RF power transfer for space solar power applications," 2018. [Online]. Available: https://arc.aiaa.org/doi/abs/10.2514/6.2018-2202

[80] Caltech, "Caltech's space-solar power project," 2020, Accessed: Dec. 10, 2021. [Online]. Available: https://www.spacesolar.caltech.edu

[81] B. Abiri et al., "A lightweight space-based solar power generation and transmission satellite," 2022. [Online]. Available: https://arxiv.org/abs/2206.08373

[82] M. Gal-Katziri, A. Fikes, F. Bohn, B. Abiri, M. R. Hashemi, and A. Hajimiri, "Scalable, deployable, flexible phased array sheets," in *Proc. IEEE/MTT-S Int. Microw. Symp.*, 2020, pp. 1085–1088.

[83] M. Gal-Katziri, C. Ives, A. Khakpour, and A. Hajimiri, "Optically synchronized phased arrays in CMOS," *IEEE J. Solid-State Circuits*, vol. 57, no. 6, pp. 1578–1593, Jun. 2022.

[84] O. H. Karabey, A. Gaebler, S. Strunck, and R. Jakoby, "A 2-D electronically steered phased-array antenna with 2 × 2 elements in LC display technology," *IEEE Trans. Microw. Theory Techn.*, vol. 60, no. 5, pp. 1297–1306, May 2012.

[85] T. Li, B. Quan, G. Fang, and T. Wang, "Flexible THz carrier-envelope phase shifter based on metamaterials," *Adv. Opt. Mater.*, vol. 10, no. 18, 2022, Art. no. 2200541. [Online]. Available: https://onlinelibrary.wiley.com/doi/abs/10.1002/adom.202200541

[86] S. I. Park et al., "Stretchable multichannel antennas in soft wireless optoelectronic implants for optogenetics," *Proc. Nat. Acad. Sci.*, vol. 113, no. 50, pp. E8169–E8177, Nov. 2016. [Online]. Available: https://doi.org/10.1073/pnas.1611769113

[87] Z. Huang et al., "Three-dimensional integrated stretchable electronics," *Nature Electron.*, vol. 1, pp. 473–480, Mar. 2018. [Online]. Available: https://doi.org/10.1038/s41928-018-0116-y

[88] K. Jawed, N. Kazem, and C. Majidi, "Soft-matter electronics and multifunctional materials with polydisperse liquid metal suspensions: Material architecture, principles, and applications to programmable matter," in *Proc. IEEE Int. Symp. Antennas Propag. USNC/URSI Nat. Radio Sci. Meeting*, 2017, pp. 417–418.

[89] X. Peng et al., "Stretchable, compressible, and conductive hydrogel for sensitive wearable soft sensors," *J. Colloid Interface Sci.*, vol. 618, pp. 111–120, 2022. [Online]. Available: https://www.sciencedirect.com/science/article/pii/S0021979722004209

[90] D. Hensley, C. Christodoulou, and N. Jackson, "A stretchable liquid metal reconfigurable monopole antenna," in *Proc. IEEE Int. Symp. Antennas Propag. North Amer. Radio Sci. Meeting*, 2020, pp. 585–586.

[91] D. Hensley, C. Christodoulou, and N. Jackson, "A stretchable liquid metal antenna array," in *Proc. IEEE Int. Symp. Antennas Propag. USNC-URSI Radio Sci. Meeting*, 2021, pp. 1777–1778.

[92] K. C. Lim, J. D. Margerum, and A. M. Lackner, "Liquid crystal millimeter wave electronic phase shifter," *Appl. Phys. Lett.*, vol. 62, no. 10, pp. 1065–1067, 1993. [Online]. Available: https://doi.org/10.1063/1.108796

[93] D. Dolfi, M. Labeyrie, P. Joffre, and J. P. Huignard, "Liquid crystal microwave phase shifter," *Electron. Lett.*, vol. 29, no. 10, pp. 926–928, 1993.

[94] S. Foo, "Liquid-crystal-tunable metasurface antennas," in *Proc. IEEE 11th Eur. Conf. Antennas Propag.*, 2017, pp. 3026–3030.

[95] C. Wu et al., "A phased array based on large-area electronics that operates at gigahertz frequency," *Nature Electron.*, vol. 4, no. 10, pp. 757–766, Oct. 2021.

[96] W. Li, M. Vaseem, S. Yang, and A. Shamim, "Flexible and reconfigurable radio frequency electronics realized by high-throughput screen printing of vanadium dioxide switches," *Microsyst. Nanoeng.*, vol. 6, no. 1, pp. 1–12, Oct. 2020. [Online]. Available: https://doi.org/10.1038/s41378-020-00194-2

[97] M. Burla et al., "500 GHz plasmonic mach-zehnder modulator enabling sub-thz microwave photonics," *APL Photon.*, vol. 4, no. 5, 2019, Art. no. 056106. [Online]. Available: https://doi.org/10.1063/1.5086868

[98] D. T. Pham, H. Subbaraman, M. Y. Chen, X. Xu, and R. T. Chen, "Light weight and conformal 2-bit, 1 phased-array antenna with cnt-tft-based phase shifter on a flexible substrate," *IEEE Trans. Antennas Propag.*, vol. 59, no. 12, pp. 4553–4558, Dec. 2011.

[99] B. D. Braaten et al., "A self-adapting flexible (SELFLEX) antenna array for changing conformal surface applications," *IEEE Trans. Antennas Propag.*, vol. 61, no. 2, pp. 655–665, Feb. 2013.
[100] X. He and M. M. Tentzeris, "In-package additively manufactured sensors for bend prediction and calibration of flexible phased arrays and flexible hybrid electronics," in *Proc. IEEE MTT-S Int. Microw. Symp.*, 2021, pp. 327–330.
[101] O. S. Mizrahi, A. Fikes, and A. Hajimiri, "Flexible phased array shape reconstruction," in *Proc. IEEE MTT-S Int. Microw. Symp.*, 2021, pp. 31–33.
[102] I. Dokmanic, R. Parhizkar, J. Ranieri, and M. Vetterli, "Euclidean distance matrices: Essential theory, algorithms, and applications," *IEEE Signal Process. Mag.*, vol. 32, no. 6, pp. 12–30, Nov. 2015. [Online]. Available: https://dx.doi.org/10.1109/MSP.2015.2398954
[103] S. I. Rutan-Bedard, C. Winkler, K. Kugler, K. M. Webb, and S. Roy, "A frequency shift key radar approach for the reconstruction of flexible phased array geometry," in *Proc. IEEE Int. Symp. Antennas Propag. USNC-URSI Radio Sci. Meeting*, 2022, pp. 1778–1779.

AUSTIN C. FIKES (Member, IEEE) received the B.S. degree in engineering from Harvey Mudd College, Claremont, CA, USA, in 2016, the M.S. degree in electrical engineering from the California Institute of Technology (Caltech), Pasadena, CA, USA, in 2018, and the Ph.D. degree from the Caltech Holistic Integrated Circuit Lab, in 2022. His research interests include decentralized, large-scale, and microwave arrays with novel form-factors.

MATAN GAL-KATZIRI (Member, IEEE) received the B.S. degree in physics and electrical engineering from Ben-Gurion University, Beer Sheva, Israel, in 2009, and the M.S. and Ph.D. degrees in electrical engineering from the California Institute of Technology (Caltech), Pasadena, CA, USA, in 2016 and 2020, respectively. He studied integrated magnetic sensors for biomedical applications and investigated high-power and low-mass antenna arrays with Caltech's SpaceSolar Power Program RF Team until 2021. Since 2021, he has been with Ben-Gurion University. His research interests include large antennas and arrays for communication, and remote-sensing applications. Dr. Gal-Katziri was the recipient of the Analog Devices Outstanding Student Designer Award in 2015 and the IMS Advanced Practice Paper Award for his work on flexible arrays transmitters in 2020.

OREN S. MIZRAHI (Student Member, IEEE) received the B.S. degree in electrical and computer engineering, the second B.S. degree in biomedical engineering, and a minor in mathematics from Duke University, Durham, NC, USA, in 2019, and the M.S. degree in electrical engineering from the California Institute of Technology (Caltech), Pasadena, CA, USA, in 2021. He is currently working toward the Ph.D. degree with Caltech Holistic Integrated Circuit Lab. His research interests include high dimensional systems, imaging, sensing, and flexible phased arrays.

D. ELLIOTT WILLIAMS (Member, IEEE) received the B.S. and M.Eng. degrees in electrical engineering and computer science from the Massachusetts Institute of Technology (MIT), Cambridge, MA, USA, in 2015 and 2016 respectively, and the Ph.D. degree in electrical engineering from the California Institute of Technology, Pasadena, CA, USA, in 2022. He joined the Faculty of Hofstra University, Hempstead, NY, USA, in 2022. His vision is to create devices with enhanced control of electromagnetic fields that can dynamically adapt to changing environments and/or needs. Previously, he was with SpaceX, Hawthorne, CA, USA, where he helped develop the phased arrays for the initial prototype Starlink satellites, and with Apple Inc., Cupertino, CA, USA, where he explored experimental technologies for new product features. His research focuses on developing adaptive electromagnetic systems using novel degrees of freedom. Dr. Williams was the recipient of the Analog Devices Outstanding Student Designer Award in 2017 and the 2022 EuMC Young Engineer Prize for his work on flexible meta-gaps.

ALI HAJIMIRI (Fellow, IEEE) received the B.S. degree in electronics engineering from Sharif University of Technology, Tehran, Iran, and the M.S. and Ph.D. degrees in electrical engineering from Stanford University, Stanford, CA, USA, in 1996 and 1998, respectively. From 1993 to 1994, he was with Philips Semiconductors, Eindhoven, The Netherlands, where he worked on a BiCMOS chipset for GSM and cellular units. In 1995, he was with Sun Microsystems, Santa Clara, CA, USA, working on the UltraSPARC microprocessors cache RAM design methodology. During summer 1997, he was with Lucent Technologies (Bell Labs), Murray Hill, NJ, USA, where he investigated low-phase-noise integrated oscillators. In 1998, he joined the Faculty of the California Institute of Technology, Pasadena, CA, USA, where he is currently a Bren Professor of electrical engineering and medical engineering, the Director of the Microelectronics Laboratory, and Co-Director of Space Solar Power Project. He has authored and coauthored more than 250 refereed journal and conference technical articles and granted more than 130 U.S. patents with many more pending applications. He is the author of *Analog: Inexact Science, Vibrant Art* (2021, Early Draft), a book on fundamental principles of analog circuit design, and *The Design of Low Noise Oscillators* (Boston, MA: Springer). His research interests include high-speed and high-frequency integrated circuits for applications in sensors, photonics, biomedical devices, and communication systems. Prof. Hajimiri is a Fellow of National Academy of Inventors, Tampa, FL, USA. He was selected to the TR35 top innovator's list. He was a Distinguished Lecturer of the IEEE Solid-State and Microwave Societies. He was the recipient of the Microwave Prize, Feynman Prize for Excellence in Teaching, Caltech's most Prestigious Teaching Honor, and Caltech's Graduate Students Council Teaching and Mentoring Award, Associated Students of Caltech Undergraduate Excellence in Teaching Award. He was the Gold Medal winner of the National Physics Competition, and the Bronze Medal winner of the 21st International Physics Olympiad, Groningen, Netherlands. He was recognized as one of the top-10 contributors to ISSCC. He was the co-recipient of the IEEE JOURNAL OF SOLID-STATE CIRCUITS Best Paper Award, International Solid-State Circuits Conference (ISSCC) Jack Kilby Outstanding Paper Award, RFIC Best Paper Award, IMS best advance practices awards, two-time co-recipient of CICC Best Paper Award, three-time winner of the IBM Faculty Partnership Award, National Science Foundation CAREER Award, and Okawa Foundation Award. In 2002, he co-founded Axiom Microdevices Inc., whose fully-integrated CMOS PA has shipped around 400,000,000 units, and was acquired by Skyworks Inc. in 2009. He is a Co-founder of GuRu Wireless Inc. He has served on the Technical Program Committee of the International Solid-State Circuits Conference (ISSCC), as an Associate Editor for IEEE JOURNAL OF SOLID-STATE CIRCUITS and IEEE TRANSACTIONS ON CIRCUITS AND SYSTEMS—Part II:Express Briefs, a member of the Technical Program Committees of the International Conference on Computer Aided Design, Guest Editor of IEEE TRANSACTIONS ON MICROWAVE THEORY AND TECHNIQUES, and Guest Editorial Board member of *Transactions of Institute of Electronics, Information and Communication Engineers of Japan (IEICE)*.